



HAL
open science

Comparison of methane yield of a novel strain of *Methanothermobacter marburgensis* in pure and mixed adapted culture derived from a methanation bubble column bioreactor

Corinne Biderre-Petit, Mbarki Mariem, Damien Courtine, Benarab Yanis, Christophe Vial, Pierre Fontanille, Pascal Dubessay, Misagh Keramati, Isabelle Jouan-Dufournel, Arthur Monjot, et al.

► To cite this version:

Corinne Biderre-Petit, Mbarki Mariem, Damien Courtine, Benarab Yanis, Christophe Vial, et al.. Comparison of methane yield of a novel strain of *Methanothermobacter marburgensis* in pure and mixed adapted culture derived from a methanation bubble column bioreactor. *Bioresource Technology*, inPress, 406, pp.131021. 10.1016/j.biortech.2024.131021 . hal-04621855v2

HAL Id: hal-04621855

<https://hal.science/hal-04621855v2>

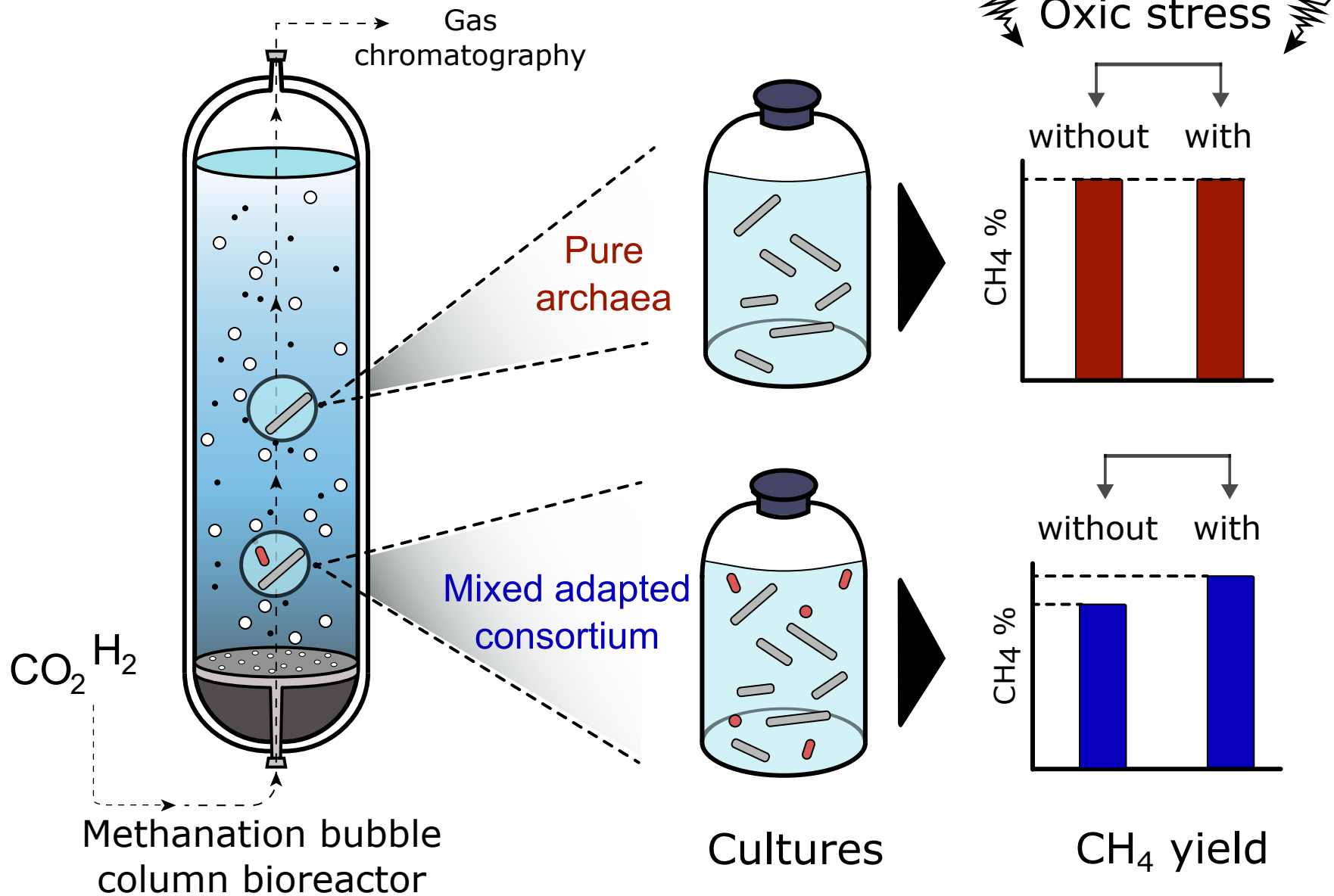
Submitted on 24 Jun 2024

HAL is a multi-disciplinary open access archive for the deposit and dissemination of scientific research documents, whether they are published or not. The documents may come from teaching and research institutions in France or abroad, or from public or private research centers.

L'archive ouverte pluridisciplinaire **HAL**, est destinée au dépôt et à la diffusion de documents scientifiques de niveau recherche, publiés ou non, émanant des établissements d'enseignement et de recherche français ou étrangers, des laboratoires publics ou privés.



Distributed under a Creative Commons Attribution - NonCommercial 4.0 International License



Highlights

1. Archaeal cell enumeration using flow cytometry
2. MBA03 association with *Methanothermobacter* as an indicator of process stability
3. O₂ exposure impacts CH₄ yield of the consortium but not that of pure strains
4. Two *Methanothermobacter marburgensis* strains with different growth behaviour

Title

Comparison of methane yield of a novel strain of *Methanothermobacter marburgensis* in pure and mixed adapted culture derived from a methanation bubble column bioreactor

Authors

Biderre-Petit Corinne^{1*}, Mbarki Mariem¹, Courtine Damien¹, Benarab Yanis¹, Vial Christophe², Fontanille Pierre², Dubessay Pascal², Keramati Misagh², Jouan-Dufournel Isabelle¹, Monjot Arthur¹, Guez Jean Sébastien² and Fadhlaoui Khaled^{1,3*}

¹Université Clermont Auvergne, CNRS, Laboratoire Microorganismes : Génome et Environnement, F-63000, Clermont-Ferrand, France.

²Université Clermont Auvergne, Clermont Auvergne INP, CNRS, Institut Pascal, 63000 Clermont-Ferrand, France.

³Université Clermont Auvergne, UMR 454 MEDIS UCA-INRAE, F-63000 Clermont-Ferrand, France

*For correspondence: Corinne Biderre-Petit, 1 Impasse Amélie Murat - Bat BioA 63178 Aubière (France). E-mail: corinne.petit@uca.fr, Tel: +33(0)473405139; Fax+33 (0)473407670; Khaled Fadhlaoui, 1 Impasse Amélie Murat - Bat BioA 63178 Aubière (France). E-mail: khaled.fadhlaoui@uca.fr, Tel: +33(0)473177959; Fax+33 (0)473407670.

E-mails: C Petit: corinne.petit@uca.fr; M Mbarki: mmbarki342@gmail.com; D Courtine: Damien.courtine@uca.fr; Y Benarab: benarabyanis0@gmail.com; C Vial: christophe.vial@uca.fr; P Fontanille: pierre.fontanille@uca.fr, P Dubessay: pascal.dubessay@uca.fr; M Keramati: Misagh.KERAMATI@uca.fr; I Jouan-Dufournel: Isabelle.JOUAN@uca.fr; A Monjot: arthur.monjot.pro@gmail.com; JS Guez: j-sebastien.guez@uca.fr; K Fadhlaoui: Khaled.fadhlaoui@uca.fr

Acknowledgements

The authors would like to acknowledge Hermine Billard and Jonathan Colombet, Plateforme SYSTEM – UCA PARTNER (Clermont-Ferrand, France), for their technical support and expertise. We also thank Pr. Cécile Lepère and Dr. Bernard Ollivier for their thorough reviewing of the manuscript.

Funding sources

This work was sponsored by the French government research program through ANR BIOMINTENS [grant number ANR-20-CE05-0031, 2021].

1 **Title**

2 Comparison of methane yield of a novel strain of *Methanothermobacter marburgensis*
3 in pure and mixed adapted culture derived from a methanation bubble column
4 bioreactor

5

6 **Abstract**

7 The ongoing discussion regarding the use of mixed or pure cultures of
8 hydrogenotrophic methanogenic archaea in Power-to-Methane (P2M) bioprocess
9 applications persists, with each option presenting its own advantages and disadvantages.
10 To address this issue, a comparison of methane (CH₄) yield between a novel
11 methanogenic archaeon belonging to the species *Methanothermobacter marburgensis*
12 (strain Clermont) isolated from a biological methanation column, and the community
13 from which it originated, was conducted. This comparison included the type strain *M.*
14 *marburgensis* str. Marburg. The evaluation also examined how exposure to oxygen (O₂)
15 for up to 240 minutes impacted the CH₄ yield across these cultures. While both
16 *Methanothermobacter* strains exhibit comparable CH₄ yield, slightly higher than that of
17 the mixed adapted culture under non-O₂-exposed conditions, strain Clermont does not
18 display the lag time observed for strain Marburg.

19

20 **Keywords**

21 *Methanothermobacter marburgensis*, mixed hydrogenotrophic methanogenic culture,
22 oxygen exposure, multi-omics approaches.

23

24 **1. Introduction**

25 To limit the rise of global surface temperature to less than 2°C while meeting the
26 increasing energy demand, a significant global energy transition is urgently needed.
27 However, shifting away from polluting fossil fuels to low-carbon solutions requires
28 technological innovation, particularly in renewable energy. Despite substantial progress
29 in wind, solar, and geothermal energies, challenges such as intermittency, variability,
30 geographical limitations, and storage persist (Tong et al., 2021). Power-To-Gas (P2G)
31 concept has emerged as a promising solution allowing the storage of surplus of
32 renewable energy recovered from the electricity sector in the form of gas (*i.e.*
33 dihydrogen (H₂) called P2H and CH₄ called P2M) (Glenk and Reichelstein, 2022).
34 Currently, P2M offers advantages over P2H. It allows converting electricity into
35 chemical energy and uses existing infrastructure. Considering storability, it has a higher
36 energy density (10 kWh/Nm³ for CH₄ versus 3 kWh/Nm³ for H₂) and is suitable for
37 long term and large-scale storage (Blanco et al., 2018). P2M systems combine H₂
38 oxidation and carbon dioxide (CO₂) reduction to produce CH₄ using either
39 physicochemical or biological catalysts (biomethanation). Comparatively,
40 biomethanation processes require lower temperatures and pressures than
41 physicochemical methanation processes and exhibit increased resistance to chemical
42 contaminants including hydrogen sulfide (H₂S), organic acids, or ammonia (Burkhardt
43 et al., 2015).
44 Hydrogenotrophic methanogenic archaea (HMs), which can use H₂ as a reducing agent
45 for the conversion of CO₂ into CH₄, are key biocatalysts for biomethane (Bellini et al.,
46 2022). They require as much H₂ as the system can provide for CO₂ reduction.
47 Therefore, the competition and sustainable equilibrium between H₂ producers (*e.g.*
48 acetogens) and consumers (*e.g.* HMs) usually result in a very low dissolved H₂ partial

49 pressure ($p(\text{H}_2)$) to maintain a balanced operation of the entire microbiological
50 community. However, numerous abiotic and biotic factors can affect this equilibrium.
51 From a thermodynamical perspective, external H_2 provision strongly favours
52 hydrogenotrophic methanogenesis. But a sudden increment of $p(\text{H}_2)$ can enable the
53 homoacetogenic pathway to outcompete the hydrogenotrophic methanogenesis (Treu et
54 al., 2018; Tsapekos et al., 2022). In addition, temperature, pH, H_2/CO_2 ratio, H_2 supply,
55 etc, are all abiotic factors that can influence CH_4 content and microbial community
56 during *in-situ* biological biogas upgrading (Rachbauer et al., 2017; Wahid et al., 2019).
57 Among HMs, the main actors in biomethanation processes comprise members of the
58 genera *Methanoculleus*, *Methanothermobacter*, *Methanobacterium*, or *Methanosarcina*.
59 The relative abundance of these genera in biogas upgrading reactors varies based on
60 factors such as temperature, pH, carbon monoxide (CO), etc (Thema et al., 2021; Xu et
61 al., 2020). In thermophilic conditions, *Methanothermobacter* was shown to be
62 predominant in the mixed cultures due to its favorable growth at higher temperatures
63 (Kaster et al., 2011; Szuhaj et al., 2021). Within this genus, *Methanothermobacter*
64 *thermautotrophicus* and *Methanothermobacter marburgensis*, largely used as model
65 organisms, have already been implemented as biocatalysts in large-scale industrial
66 processes because they are robust, and reach high cell densities, and CH_4 production
67 rate (Seifert et al., 2014; Pfeifer et al., 2021; Thema et al., 2021, Kaul et al., 2022).
68 Two main approaches can be employed for biomethanation, *i.e.* using pure cultures or
69 enriched mixed cultures, each with its own advantages and drawbacks (Rachbauer et al.,
70 2017; Rafrafi et al., 2021; Rittmann et al., 2018). Indeed, using single self-replicating
71 catalysts would prevent oxidation of H_2 by other hydrogenotrophic microorganisms,
72 thereby avoiding a loss of efficiency in biogas upgrading. It would also allow for better

73 system variability and behaviour prediction (Martin et al., 2013). On the other hand,
74 using consortia would be more efficient, leading to larger CH₄ yields (Bellini et al,
75 2022, Paniagua et al., 2022). Other advantages of employing consortia include greater
76 robustness and short recovery time upon starvation/excess input gas rate and
77 oxygenation. However, managing mixed cultures often requires increased control and a
78 thorough understanding of how microbial composition impacts the system (Paniagua et
79 al., 2022). Therefore, despite the growing number of studies in this field, the question of
80 whether pure or mixed cultures are more suitable for biomethanation processes remains
81 unresolved. To address this question, a comparison of the performance of both HM pure
82 cultures and reactor microbiomes from which HMs have been isolated appears essential.
83 This study aims to evaluate the methanation efficiency of a new HM affiliated to the *M.*
84 *marburgensis* species (strain Clermont) isolated from a bubble column reactor. Its
85 methanogenic performance was compared not only with its native consortium but also
86 with the type strain, *i.e.* *M. marburgensis* strain Marburg (hereinafter referred to as
87 strain Marburg). This comparison was extended under oxidative stress, a common
88 occurrence in biomethanation processes.

89

90 **2. Material and Methods**

91 **2.1. Laboratory-scale methanation reactor**

92 The mixed adapted culture used in this study was collected from a 3.5 L bubble column
93 reactor, six weeks after its inoculation with 300 mL of digestate from a thermophilic
94 industrial-scale biogas plant treating livestock effluent and agri-food industry wastes
95 that operates between 52 and 54°C (Methelec, Ennezat, France). Briefly, the reactor
96 contained 2.7 L of basal anaerobic (BA) culture medium prepared as previously
97 reported (Bu et al., 2018) and reduced by introducing 0.4 g/L of sodium sulfide

98 nanohydrate ($\text{Na}_2\text{S}\cdot 9\text{H}_2\text{O}$). The H_2/CO_2 gas mixture was set at a ratio of 4:1 (v/v) with a
99 mass flowmeter (SLA5800, Brooks Instrument, Hatfield, USA). Flow rates ranged from
100 0.29 to 0.44 $\text{NL}\cdot\text{min}^{-1}$. The temperature was set to 55°C using a thermostatic bath (Eco
101 RE1225 silver, Lauda, Königshofen, Germany).

102 Volatile fatty acids (VFAs) in the six-week mixed adapted culture were determined
103 using a liquid chromatograph (1260 HPLC, Agilent, Santa Clara, USA). The HPLC
104 apparatus was equipped with two columns (Rezex ROA 300 x 7.8 nm, Phenomenex,
105 Torrance, USA) mounted in serial in an oven (50°C) and coupled with a refractive index
106 detector. The mobile phase was a 2 mM sulfuric acid in ultra-pure water pumped at 0.7
107 $\text{mL}\cdot\text{min}^{-1}$ and 70 bars. For the analysis, 2 mL of sample were mixed with 125 μL of
108 $\text{Ba}(\text{OH})_2\cdot 8\text{H}_2\text{O}$ (0.3 M) and 125 μL of $\text{ZnSO}_4\cdot 7\text{H}_2\text{O}$ (5% w/v) before a 5 min
109 centrifugation at 10000 g. Samples were filtered through 0.2 μm nylon filters before
110 being injected in the HPLC apparatus.

111 Measurements of archaeal and bacterial abundance (quantitative real-time PCR),
112 performed on the six-week sample mixed adapted culture, revealed a dominance of
113 archaea over bacteria with an archaea/bacteria ratio of five ($1.0\ 10^9$ archaeal cells/mL
114 versus $2.2\ 10^8$ bacterial cells/mL).

115 **2.2. Microbial community analysis of the mixed adapted culture**

116 Two mL of the six-week mixed adapted culture were centrifuged at 10000 g at room
117 temperature (RT) for 10 min and total genomic DNA (gDNA) was extracted from the
118 pellet using a Nucleo Spin Soil kit in accordance with manufacturer's instructions
119 (Machery Nagel, Düren, Germany). Then, gDNA was quantified using a
120 spectrophotometer (NanoDrop 1000, Thermo Fisher Scientific, USA). Subsequently,
121 the V3-V4 hypervariable region of the bacterial 16S ribosomal RNA (rRNA) genes was

122 amplified using the primer set F343 (5'-
123 CTTTCCCTACACGACGCTCTTCCGATCTACGGRAGGCAGCAG-3') - R784 (5'-
124 GGAGTTCAGACGTGTGCTCTTCCGATCTTACCAGGGTATCTAATCCT-3')
125 (Carmona-Martinez et al., 2015) while the V4-V5 region of the archaeal 16S rRNA
126 genes was amplified with the primer set F504-519 (5'-
127 CTTTCCCTACACGACGCTCTTCCGATCTCAGCMGCCGCGGKAA-3') and R910-
128 928 (5'-GGAGTTCAGACGTGTGCTCTTCCGATCTCCCGCCWATTCCTTTAAGT-
129 3') (Braga Nan et al., 2020), primers containing adapters and barcodes for Miseq
130 sequencing. PCR reactions contained TaqTM TaKaRa Premix, 1 µM of each primer, 200
131 µM of each deoxynucleoside triphosphate (dNTP), 0.625 U TaKaRa Taq polymerase
132 (TakaRa Inc., France), nuclease free-H₂O and 50 to 100 ng gDNA template in a total
133 volume of 50 µL. For both bacteria and archaea, after a denaturation step of 1 min at
134 98°C, PCR steps at 98°C for 1 min, 59°C for 40 s, and 72°C for 1 min were repeated 35
135 times, followed by an elongation step at 72°C for 10 min in a Mastercycler® thermal
136 cycler (Eppendorf, Hamburg, Germany). Amplicon size was checked by Agilent High
137 Sensitivity DNA Kit on 2100 Bioanalyzer (Agilent Technologies, Santa Clara, CA,
138 USA). Amplicon libraries were prepared and sequenced by the GenoToul platform
139 (Toulouse, France) with an Illumina MiSeq sequencer to generate 2 x 300 bp paired-end
140 reads. Bacterial and archaeal reads were separately processed using a homemade
141 bioinformatics pipeline. Briefly, paired reads were merged using the VSEARCH
142 v2.18.0 (Rognes et al., 2016) and then trimmed and filtered with Cutadapt (Martin,
143 2011) to minimize the effects of random sequencing errors as follows: (i) only merged
144 reads with a length 200-500 bp were kept, (ii) paired reads with sequencing errors in
145 primers were discarded and (iii) primer sequences and nucleotides with Phred quality

146 scores upper than 30 were trimmed. Deletion of chimeric sequences and clusterization
147 were carried out using VSEARCH (Rognes et al., 2016) and operational taxonomic
148 units (OTUs) that accounted for <0.005% of the total set of sequences were discarded
149 (Bokulich et al., 2013). The taxonomic assignment was performed against the SILVA
150 v138.1 SSU NR99 database using the global alignment script in VSEARCH (Pruesse et
151 al, 2007; Rognes et al., 2016).

152 **2.3. Hydrogenotrophic methanogenic archaea isolation and analytical procedures**

153 A serum vial (Dutscher, Bernolsheim, France) containing 50 ml of BA medium (110
154 mL in capacity) was inoculated with an aliquot of the six-week mixed adapted culture
155 (10% v/v). After BA medium autoclaving, and prior to its inoculation, dinitrogen (N₂)
156 filling the head space was replaced by H₂/CO₂ (4:1, v/v) gas mixture from a gas
157 cylinder (Westfalen, France) at 2 bars. Liquid cultivation was conducted at 55°C in the
158 dark, without agitation.

159 HM isolation was performed *via* successive dilution to extinction series in Hungate
160 tubes (16.5 mL capacity) containing 5 mL of either liquid or solid BA medium (2% agar
161 w/v; roll-tube technique (Hungate, 1969)). Headspace composition was determined by
162 gas chromatography (3000A MicroGC, Agilent Technologies, Santa Clara, CA, USA)
163 equipped with two capillary columns (one MS-5A column associated with a backflush
164 injector and one PorapLOT Q column associated with a standard injector) and Soprane
165 software v3.5.2 for the analysis. The microGC used argon as gas carrier and the
166 temperature of the columns and injectors were at 50 and 60°C, respectively.

167 The purity of HMs was checked by microscopic observations (Leica DM IRB inverted
168 microscope equipped with a Hamamatsu C13440 camera and Zen Blue v3.1 software)
169 and by adding yeast extract (2 g/L) and glucose (20 mM final concentration) to the BA

170 medium to confirm the absence of fermentative bacteria. Subsequently, HM taxonomic
171 identification was performed by 16S rRNA gene sequence amplification using the
172 universal primer set Arch21F-1492R (Nakagawa et al., 2006) followed by sequencing
173 (Eurofins Genomics, Cologne, Germany). For the ultrastructural characterization, the
174 archaeal cells in 1% (v/v) formaldehyde fixed samples were collected by centrifugation
175 at 20000 g for 20 min at 14°C directly onto 400-mesh electron microscopy copper grids
176 covered with carbon-coated Formvar film (AO3X, Pelanne Instruments, Toulouse,
177 France). Particles were over contrasted with 2% uranyl salts and rinsed three times in
178 distilled deionized water before being dried at RT. Subsequently, the characterization
179 was performed with a transmission electron microscope using a JEOL 2100
180 (Akishikma, Tokyo, Japan; Plateforme CYSTEM, UCA Partner, Clermont-Ferrand,
181 France). The microscope was operated at 80 kV, and the images were recorded with an
182 Gatan CMOS RIO 9 camera (Gatan Ametek, Pleasanton, USA) at 3072 x 3072 pixels.
183 Since all HMs belonged to the same strain, one representative, called
184 *Methanothermobacter marburgensis* strain Clermont (hereafter referred to as strain
185 Clermont), was deposited in the Deutsche Sammlung von Mikroorganismen und
186 Zellkulturen (DSMZ) culture collection (accession number DSM 34405).

187 **2.4. Cultivation procedures**

188 The hydrogenotrophic and methanogenic activities of strain Clermont, the mixed
189 adapted culture, and *M. marburgensis* strain Marburg obtained from DSMZ (DSM
190 2133), which is the closest relative of strain Clermont (99.5% 16S rRNA gene identity),
191 were investigated under reduced conditions. Cultures were conducted in serum vials
192 containing 50 mL of BA medium as described above (Paragraph 2.3). All inoculations
193 were performed with the same number of archaeal cells, *i.e.* 5.7×10^5 cells. Briefly, an

194 aliquot of 1 mL of pure or mixed cultures at the end of the exponential growth phase
195 was diluted to 1:10 and directly used for flow cytometry analysis (BD LSR Fortessa X-
196 20; BD Biosciences, CA, USA). Two lasers (Violet, 405 nm, 50 mW and Blue, 488 nm,
197 60 mW) were used for F420 cofactor excitation (autofluorescence of archaeal cells) and
198 morphological characterization, respectively. The threshold was set at 200 on the F420
199 cofactor parameter. Data were acquired during 60 sec at a constant flow rate of 29.85
200 $\mu\text{L}/\text{min}$ and processed using FACSDivA 9 software (BD Biosciences).

201 Cultures subjected to oxidative stress were inoculated and grown in medium devoid of
202 chemical reducing agents, namely $\text{Na}_2\text{S}\cdot 9\text{H}_2\text{O}$ and resazurin, generally used to reinforce
203 anaerobiosis and detect any potential oxidation, to prevent O_2 reduction during the
204 exposure. Indeed, their presence would have reduced the effective amount of O_2 during
205 oxic stress. Anaerobiosis prior to oxic stress was confirmed by microGC. After reaching
206 the end of the exponential growth phase in anaerobic conditions, the cultures were
207 transferred to sterile beakers in a laminar flow hood and placed under high stirring
208 speed to be exposed to atmospheric levels of O_2 (21%) for durations of 0, 10, 30, 60, 90,
209 120, and 240 min. The quantity of dissolved O_2 measured in the medium was $10 \text{ mg/L} \pm$
210 0.32 mg/L from 1 min up to 240 min of exposure (portable oximeter, Laqua 200 series,
211 Horiba Scientific, Japan). Subsequently, fresh BA medium containing a reducing agent
212 was inoculated as above. The absence of O_2 was checked by gas chromatography before
213 incubation.

214 All experiments were conducted in biological triplicates. During growth, gas
215 composition in the headspace was monitored daily by gas chromatography. Statistical
216 analysis of CH_4 yield during growth was conducted using the Student t-test, one-way or
217 two-way ANOVA (culture \times incubation days) followed by Tukey's test under normality

218 and homoscedasticity assumption. The level of significance was set at $\alpha=0.05$. All
219 statistical analyses were performed using the R Stats package v4.2.2.

220 **2.5. DNA extraction for whole genome sequencing of the *M. marburgensis* strain**

221 **Clermont**

222 A culture of strain Clermont (50 mL) in exponential growth was concentrated by
223 centrifugation for 15 min at 10000 g at RT. gDNA was extracted from the pellet using a
224 standard phenol–chloroform method (Biderre-Petit et al, 2024) before quantification on
225 a Qubit Fluorometer (ThermoFisher Scientific, USA) by using QubitTM dsDNA HS
226 assay kit in accordance with manufacturer’s instructions. Subsequently, 300 ng of
227 gDNA were sequenced using Illumina HiSeq technology (2 × 150 bp; Eurofins
228 Genomics, Constance, Germany). Raw paired-end reads were quality-filtered with fastp
229 v0.23.4 (Chen et al., 2018). *De novo* assembly of whole genome sequencing data was
230 performed using Unicycler v0.5.0 (Wick et al., 2017) with default settings. In the
231 following step, the short contigs with viral/transposable elements (BLASTX search
232 against non-redundant database) and fragmented rRNA operons (barrnap v0.9 and
233 parameter "--kingdom arc", <https://github.com/tseemann/barrnap>) were filtered out.

234 **2.6. Phylogenomic tree construction**

235 Representative genomes of *Methanothermobacterium*, *Methanonatronarchaeia*,
236 *Archaeoglobi*, *Methanobacteria*, *Methanococci*, *Methanomicrobia*, *Methanopyri*,
237 *Thermococci*, and *Halobacterium* were downloaded from the National Center for
238 Biotechnology Information (NCBI) RefSeq. Subsequently, a genome-based
239 phylogenetic tree was generated with the program GToTree v1.8.2 as reported in
240 Biderre-Petit et al. (2024), using an archaea-specific gene set composed of 73 markers.
241 Individual gene alignments were concatenated to construct a species tree using IQ-

242 TREE v2.2.3 with the evolution model LG+F+I+R10 and parameters "-B 2000 --alrt
243 2000 --bnni" (Minh et al., 2020). *Halobacterium* was used as an outgroup.

244 **2.7. Pan-genomic analysis and other genome characterizations**

245 Pan-genomic analysis of the Marburg clade (*i.e.* including the strains Marburg,
246 Clermont and their closest relatives-strain KEPCO-1 (assembly accession
247 GCA_008033705.1), strain K4 (GCA_022014235.1), strain THM2
248 (GCA_009917665.1), bin GMQ_75_MeOH_H2_bin_21 (GCA_030055425.1) and bin
249 JZ-3_D_bin_25 (GCA_030055435.1); seven genomes in total) was carried out using the
250 "pan-genomics workflow of anvi'o v7.1 (Delmont and Eren, 2018). The average
251 nucleotide identity (ANI) was also calculated through anvi'o and to complete the
252 results, *in silico* DNA-DNA hybridization (*isDDH*) was computed using Genome-to-
253 Genome Distance Calculator v2.1 with formula 2 as previously recommended (Meier-
254 Kolthoff et al., 2013). Genome synteny was visualized by NGenomeSyn v1.41 (He et
255 al., 2023).

256

257 **3. Results and discussion**

258 **3.1. Overview of microbial community diversity in a bubble column reactor**

259 Metabarcoding procedure was used to separately address the archaeal and bacterial
260 diversity present in the six-week adapted culture. Although less abundant than archaea,
261 bacteria showed much higher diversity, with 833 OTUs (19403 reads in total) versus 42
262 OTUs (28482 reads), respectively, which is consistent with what is generally described
263 for mixed cultures (Xu et al., 2020). For the archaea, the four most abundant OTUs
264 (>1% relative abundance in the sample) covered 96.1% of the community (See
265 supplementary material). *Methanothermobacter* genus represented 98.5% of the

266 archaeal community in terms of reads, followed by *Methanobacterium* (1.2%),
267 *Methanomassiliicoccus* (0.09%) and *Methanoculleus* (0.01%) (Fig. 1A). This finding
268 closely aligns with previous research, which has shown that *Methanothermobacter* is
269 the dominant genus in the hydrogenotrophic methanogenic consortium of *ex-situ*
270 methanation systems at 55°C (Xu et al., 2020). Within this genus, 98.9% of the reads
271 are affiliated to the *M. marburgensis* species (>97% 16S rRNA gene sequence identity).
272 Regarding bacteria, the most represented phyla in terms of reads were *Bacillota* (ex
273 *Firmicutes*, 91.8% of total bacterial reads) followed by *Pseudomonadota* (ex
274 *Proteobacteria*, 6.8%) (Fig. 1B), in agreement with previous studies (Bassani et al.,
275 2015; Campanaro et al., 2020). The 11 most abundant OTUs (>1% relative abundance
276 in the sample) covered 48.7% of the bacterial community (See supplementary material)
277 and mostly affiliated with the genus *Haloplasma* (35.2% of all bacterial reads) and the
278 class *Limnochordia* (33.2%) in *Bacillota*.
279 The most abundant taxon, *i.e.* *Haloplasma*, is currently represented by only one
280 representative, a halophilic bacterium isolated from a deep-sea brine lake, named *H.*
281 *contractile*. The growth limit of this bacterium was determined at 44°C (Antunes et al.,
282 2008), which is not in accordance with the temperature used in this study, *i.e.* 55°C.
283 However, although SILVA classifies this predominant taxon in the genus *Haloplasma*,
284 the sequence used as reference and which shows 99% identity with OTUs affiliated to
285 *Haloplasma* (accession number FN436037, see supplementary material), displays only
286 up to 89% sequence similarity with *Haloplasma* using BLAST N against the nucleotide
287 database in NCBI. This may be due to the low number of sequences representative of
288 the genus *Haloplasma* and also more generally of the family and order. Indeed, the
289 order Haloplasmatales currently includes a single family -Haloplasmataceae- which

290 includes a single genus and species: *H. contractile*. This most likely not only leads to an
291 inaccurate affiliation at the genus level, but also potentially at the family level.
292 Consequently, the representatives that will be discovered for this group of
293 Haloplasmodiales will most certainly allow significant changes to the current description
294 made for the single type species.

295 The second most abundant taxon, the *Limnochordia* class, is frequently observed in full-
296 size and laboratory-scale thermophilic biogas reactors (Campanaro et al., 2020). The
297 main representative in this class was MBA03 (14.6% of all bacterial reads).
298 Laguillaumie et al. (2022) suggested that MBA03, referenced as a carbohydrate
299 fermentative taxon, would grow on lysis products and prevent side products, such as
300 VFAs, from accumulating in the reactor. The low amount of VFAs measured in the
301 reactor could therefore be explained, at least in part, by the MBA03 abundance. This
302 low quantity also indicates that hydrogenotrophic methanogenesis has not shifted
303 towards homoacetogenesis. Moreover, MBA03 association with *Methanobacterium* was
304 described as an indicator of process stability (Laguillaumie et al., 2022). Its association
305 with *Methanothermobacter* could therefore still be such an indicator.

306 In addition to MBA03, two other bacteria known to be syntrophic acetate oxidizing, *i.e.*
307 *Tepidiphilus* (*Pseudomonadota*) and norank order D8A-2 (*Bacillota*), showed
308 significant relative abundance, with 2.9% and 3.6% of all bacterial reads, respectively.
309 These results are in line with previous studies, which showed that these taxa were
310 abundant in thermophilic samples and worked synergistically with HMs, providing the
311 substrates they need towards biogas production (Tang et al., 2008; Xu et al., 2020). An
312 anaerobic digestion system seeded from manure samples (which is comparable to what
313 was used for the bioreactor, *i.e.* a biogas plant treating livestock effluent) and running at

314 55°C (Sun et al., 2015), was shown to be populated with similar microbial taxa. This
315 supports the view that temperature, but also inoculum, are crucial variables in
316 determining the structure of microbial consortia in hydrogenotrophic methanogenic
317 mixed cultures (Xu et al., 2020).

318 **3.2. Isolation and genome sequencing of *M. marburgensis* strain Clermont**

319 The strain isolated from the bioreactor belonged to the genus *Methanothermobacter* and
320 showed >99.5% identity with strain Marburg 16S rRNA gene sequence (accession
321 number NR_102881.1). It was named *M. marburgensis* strain Clermont and deposited
322 in the DSMZ collection (DSM 34405). This strain was rod-shaped (~5 µm long and 0.6
323 µm wide) and non-motile (See supplementary material).

324 The draft genome of strain Clermont (~330-fold coverage), featuring six contigs (from
325 ~21.9 to 776.9 kb), had a total length of ~1.72 Mb, a N50 contig length of 593 kb, and
326 a G+C content of 48.7%. The number of coding DNA sequences was 1805 with two
327 16S-23S rRNA gene clusters, three 5S rRNA genes and 37 transfer RNA (tRNA) genes.
328 No extra-chromosomal genetic elements were detected. Genome fragmentation was
329 mainly due to the high conservation degree between rRNA operons and transposase
330 sequences that hamper the assembly tool to resolve these loci. Phylogenomic analysis
331 confirmed the close relationship of strain Clermont with strain Marburg but also with
332 three other *Methanothermobacter* strains (*i.e.* KEPCO-1, THM_2, and K4) and two bins
333 (*i.e.* GMQ_75_MeOH_H2_bin_21 and JZ-3_D_bin_25). They all formed a clade
334 (hereinafter referred to as Marburg clade) within the genus *Methanothermobacter* (Fig.
335 2A). Their genomes revealed a high degree of synteny (Fig. 2B). Based on ANI and
336 *is*DDH values, strains Clermont, Marburg, KEPCO_1 and THM_2 formed a single
337 species (ANI ≥96% and DDH ~70%; thresholds proposed for species definition

338 (Lindsey et al., 2023)) while strain K4 and the bins represented three novel
339 *Methanothermobacter* species (Fig. 2C).
340 At the pan-genome level, the Marburg clade comprised 2076 gene clusters (GCs) with
341 1564 (75.3%) forming the core genome (shared by all seven genomes), 324 (15.6%)
342 constituting the accessory genome (specific to a subset of genomes) and 188 (9.1%)
343 being unique to a single genome (Fig. 2C). The core genome contained the full suite for
344 proteins encoded to carry out the hydrogenotrophic pathway. Members of this clade can
345 assimilate acetyl-coA *via* the CO-methylating acetyl-CoA synthase from methyl-
346 tetrahydromethanopterin. In strain Marburg, this complex was also shown to play a key
347 role in CO oxidation (Diender et al., 2016). Moreover, the presence of all genes
348 involved in carboxydutrophic methanogenesis in all Marburg clade genomes suggests
349 they are also able to grow with CO as the sole carbon source. A protein of the carbonic
350 anhydrase family (Cah), known to potentially convert bicarbonate into bioavailable
351 CO₂, was also present. Finally, as strains Clermont and Marburg were unable to grow
352 on formate as an energy source (data not shown), the function of the formate
353 dehydrogenase (FdhAB) is likely to reduce CO₂ to formate for its use in the purine
354 synthesis (Kaster et al, 2011).

355 **3.3. Comparison of CH₄ yields between the pure cultures-strains Clermont and** 356 **Marburg-, and the mixed adapted culture**

357 ***3.3.1. CH₄ yield during growth under reduced conditions***

358 The isolation of a new strain for the species *M. marburgensis* (strain Clermont) from a
359 reactor microbiome enabled to compare CH₄ yield not only between two strains of the
360 same species but also between strain Clermont and the community from which it was
361 isolated. In this respect, a flow cytometry method based on the cofactor F420

362 fluorescence (Lambrecht et al., 2017) was used for quantification and each culture was
363 inoculated with 5.7×10^5 archaeal cells. The maximum specific growth rates (μ_{MAX})
364 were 0.017, 0.03 and 0.02 h^{-1} for strain Clermont, Marburg and the mixed adapted
365 culture, respectively.

366 Methanogenic activity was observed at one-day post-inoculation for strain Clermont
367 and the mixed adapted culture (Fig. 3). CH_4 yield increased linearly until total H_2
368 conversion, reaching a maximum value after six days of growth, corresponding to
369 $54.3\% \pm 1.4\%$ CH_4 in the gas fraction for strain Clermont and to $49.3\% \pm 2.6\%$ for the
370 mixed adapted culture ($p < 0.05$). This aligns with the view that the use of unique, self-
371 replicating catalysts would avoid a loss of efficiency in biogas upgrading due to H_2
372 oxidation by other hydrogenotrophic microorganisms (Martin et al, 2013).

373 For strain Marburg, methanogenic activity was observed three days post-inoculation,
374 *i.e.* with a two-day lag phase compared with strain Clermont. Total H_2 conversion was
375 observed after eight days of growth, resulting in a maximum of $53.9\% \pm 2.4\%$ CH_4 in
376 the gas fraction, a proportion similar to that obtained for strain Clermont (Fig. 3,
377 $p > 0.05$). Consequently, the medium used in this study (*i.e.* BA medium), which is that
378 used for the isolation of strain Clermont, favoured the growth behaviour of the latter but
379 not its CH_4 yield. As the two pure strains are genetically very close, one explanation of
380 the two-day delay for strain Marburg may be, in part, attributed to their accessory
381 genomes. Indeed, the genome of strain Clermont contains 121 genes that are not present
382 in strain Marburg while the genome of strain Marburg contains 49 genes not found in
383 strain Clermont, all mostly organized into clusters (the largest contained 34 genes for
384 strain Clermont while 11 genes, for strain Marburg; See supplementary material).

385 Among these accessory genes, those encoding glycosyltransferases associated with the

386 synthesis and glycosylation of cellular surface proteins (*e.g* RafB, WcaA, WcaE) were
387 more abundant in strain Clermont (See supplementary material). Kaster et al. (2011)
388 suggested that these protein families might be partially responsible for the observed
389 differences in growth rate phenotype between strain Marburg and *M.*
390 *thermautotrophicus*. If this hypothesis proves to be true, it could also partly account for
391 the observed phenotypic differences between strains Clermont and Marburg.

392 **3.3.2. CH₄ yield following oxidative stress**

393 As methanation reactors can experience episodic oxygenation (accidents, maintenance
394 operations), it is essential to assess the HMs ability to maintain CH₄ yield after exposure
395 to O₂. This has never been done for *Methanothermobacter* species, either in pure or
396 mixed cultures. Interestingly, the results showed that O₂ exposure had no impact on the
397 pure strains (*i.e.* strains Clermont and Marburg) as they exhibited the same CH₄ yield
398 levels when all H₂ was consumed (*e.g.* 51.2% ± 1.6% and 55.3% ± 2.3%, respectively;
399 after 240 min of O₂ exposure, Fig. 4B), whatever the time of exposure to O₂, *i.e* from 0
400 min up to 240 min (p>0.05; See supplemental material). The O₂ resistance capacity of
401 these strains is suspected to be mediated by the presence in their genome of energy-free
402 reactive oxygen species (ROS) scavengers of various protection enzymes, *i.e.*
403 superoxide dismutase (SOD), superoxide reductase (SOR), F₄₂₀H₂₀ oxidase (FprA),
404 peroxiredoxin (PRX), and rubrerythrin (Rbr) (Fig. 5), as previously reported for other
405 methanogens (Liu et al., 2022). However, no catalase-encoding gene was found, similar
406 to what was observed by Lyu and Lu (2018) in the Class I methanogens (*i.e.*
407 *Methanobacteriales*, *Methanocellales* and *Methanopyrales*) to which
408 *Methanothermobacter* spp. belongs. In all Marburg clade genomes, most ROS
409 scavengers co-localize with genes encoding protection enzymes like rubredoxin (Rub,

410 electron providers to SOD and SOR), ferritin (FtnA, iron detoxifier during transient O₂)
411 (Fig. 5) and F390-synthetase which is thought to have a regulatory function in O₂ stress
412 response (Vermeij et al., 1997). As most of these genes are up-regulated during the
413 growth of strain Marburg on CO, it was hypothesized that they respond to redox stress
414 in general, and not just to O₂ stress, or are regulated by universal stress proteins
415 (Diender et al., 2016). Moreover, strain Marburg still shows the same two-day lag
416 compared with strain Clermont. Its growth behaviour is therefore not altered by oxic
417 stress either.

418 Conversely, exposure to O₂ has an impact on CH₄ yield by the mixed adapted culture.
419 Indeed, it exhibited a slight increase from the sixth day of incubation, when all H₂ was
420 converted, with 50.1% ± 1.6% CH₄ yield at 240 min of O₂ exposure (Fig. 4A) versus
421 46.4% ± 2.9% at 0 min (p<0.02; See supplementary material), thereby reaching the
422 level of the pure cultures (Fig. 4B). This gap in CH₄ yield could be associated with the
423 inhibition of hydrogenotrophic microorganisms, other than strain Clermont, present in
424 the mixed adapted culture.

425

426 **4. Conclusions**

427 Although methanogenesis is well studied, gaps remain in the understanding of
428 biomethanation, particularly regarding the choice between pure and mixed cultures in an
429 energy bioprocess. Comparative analysis of bioenergetic performances between strain
430 Clermont and its native consortium shows that the pure strain outperforms the
431 consortium in CH₄ yield under reduced conditions. However, this is no longer the case
432 after exposure to O₂. Furthermore, although both pure strains show the same CH₄ yield,

433 strain Clermont displays a higher reaction speed than the type strain of its species under
434 the culture conditions used in this study.

435

436 E-supplementary data of this work can be found in online version of the paper.

437

438 **Data availability**

439 The raw reads of the 16S rRNA gene sequencing and genomic data were deposited at
440 the NCBI database under the BioProject PRJNA1044399. *M. marburgensis* strain
441 Clermont was deposited in the DSMZ German Collection of Microorganisms under
442 accession number DSM 34405. Although the strain is not in the DSMZ catalogue or
443 website, it is available on demand.

444

445 **References**

- 446 Antunes, A, Rainey, F.A., Wanner, G., Taborda, M., Pätzold, J., Nobre, M.F., da Costa,
447 M.S., Huber, R., 2008. A new lineage of halophilic, wall-less, contractile
448 bacteria from a brine-filled deep of the Red Sea. *J. Bacteriol.* 190, 3580-3587.
449 [https://doi.org/ 10.1128/JB.01860-07](https://doi.org/10.1128/JB.01860-07)
- 450 Bassani, I., Kougias, P.G., Treu, L., Angelidaki, I., 2015. Biogas Upgrading via
451 Hydrogenotrophic Methanogenesis in Two-Stage Continuous Stirred Tank
452 Reactors at Mesophilic and Thermophilic Conditions. *Environ. Sci. Technol.* 49,
453 12585–12593. <https://doi.org/10.1021/acs.est.5b03451>
- 454 Bellini, R., Bassani, I., Vizzarro, A., Azim, A., Vasile, N., Pirri, C., Verga, F., Menin,
455 B., 2022. Biological Aspects, Advancements and Techno-Economical

456 Evaluation of Biological Methanation for the Recycling and Valorization of
457 CO₂. *Energies* 15, 4064. <https://doi.org/10.3390/en15114064>

458 Biderre-Petit, C., Courtine, D., Hennequin, C., Galand, P.E., Bertilsson, S., Debroas, D.,
459 Monjot, A., Lepère, C., Divne, A., Hochart, C., 2024. A pan-genomic approach
460 reveals novel *Sulfurimonas* clade in the ferruginous meromictic Lake Pavin.
461 *Mol. Ecol. Resour.* e13923. <https://doi.org/10.1111/1755-0998.13923>

462 Blanco, H., Nijs, W., Ruf, J., Faaij, A., 2018. Potential of Power-to-Methane in the EU
463 energy transition to a low carbon system using cost optimization. *Appl. Energy*
464 232, 323–340. <https://doi.org/10.1016/j.apenergy.2018.08.027>

465 Bokulich, N.A., Subramanian, S., Faith, J.J., Gevers, D., Gordon, J.I., Knight, R., Mills,
466 D.A., Caporaso, J.G., 2013. Quality-filtering vastly improves diversity estimates
467 from Illumina amplicon sequencing. *Nat. Methods* 10, 57–59.
468 <https://doi.org/10.1038/nmeth.2276>

469 Braga Nan, L., Trably, E., Santa-Catalina, G., Bernet, N., Delgenès, J.-P., Escudié, R.,
470 2020. Biomethanation processes: new insights on the effect of a high H₂ partial
471 pressure on microbial communities. *Biotechnol. Biofuels* 13, 141.
472 <https://doi.org/10.1186/s13068-020-01776-y>

473 Bu, F., Dong, N., Kumar Khanal, S., Xie, L., Zhou, Q., 2018. Effects of CO on
474 hydrogenotrophic methanogenesis under thermophilic and extreme-thermophilic
475 conditions: Microbial community and biomethanation pathways. *Bioresour.*
476 *Technol.* 266, 364–373. <https://doi.org/10.1016/j.biortech.2018.03.092>

477 Burkhardt, M., Koschack, T., Busch, G., 2015. Biocatalytic methanation of hydrogen
478 and carbon dioxide in an anaerobic three-phase system. *Bioresour. Technol.* 178,
479 330–333. <https://doi.org/10.1016/j.biortech.2014.08.023>

480 Campanaro, S., Treu, L., Rodriguez-R, L.M., Kovalovszki, A., Ziels, R.M., Maus, I.,
481 Zhu, X., Kougias, P.G., Basile, A., Luo, G., Schlüter, A., Konstantinidis, K.T.,
482 Angelidaki, I., 2020. New insights from the biogas microbiome by
483 comprehensive genome-resolved metagenomics of nearly 1600 species
484 originating from multiple anaerobic digesters. *Biotechnol. Biofuels* 13, 25.
485 <https://doi.org/10.1186/s13068-020-01679-y>

486 Carmona-Martínez, A.A., Trably, E., Milferstedt, K., Lacroix, R., Etcheverry, L.,
487 Bernet, N., 2015. Long-term continuous production of H₂ in a microbial
488 electrolysis cell (MEC) treating saline wastewater. *Water Res.* 81, 149–156.
489 <https://doi.org/10.1016/j.watres.2015.05.041>

490 Chen, S., Zhou, Y., Chen, Y., Gu, J., 2018. fastp: an ultra-fast all-in-one FASTQ
491 preprocessor. *Bioinformatics* 34, i884–i890.
492 <https://doi.org/10.1093/bioinformatics/bty560>

493 Delmont, T.O., Eren, A.M., 2018. Linking pangenomes and metagenomes: the
494 *Prochlorococcus* metapangenome. *PeerJ.* 6, e4320.
495 <https://doi.org/10.7717/peerj.4320>

496 Diender, M., Pereira, R., Wessels, H.J.C.T., Stams, A.J.M., Sousa, D.Z., 2016.
497 Proteomic Analysis of the Hydrogen and Carbon Monoxide Metabolism of
498 *Methanothermobacter marburgensis*. *Front. Microbiol.* 7.
499 <https://doi.org/10.3389/fmicb.2016.01049>

500 Glenk, G., Reichelstein, S., 2022. Reversible Power-to-Gas systems for energy
501 conversion and storage. *Nat. Commun.* 13, 2010.
502 <https://doi.org/10.1038/s41467-022-29520-0>

503 He, W., Yang, J., Jing, Y., Xu, L., Yu, K., Fang, X., 2023. NGenomeSyn: an easy-to-
504 use and flexible tool for publication-ready visualization of syntenic relationships
505 across multiple genomes. *Bioinformatics* 39, btad121.
506 <https://doi.org/10.1093/bioinformatics/btad121>

507 Hungate, R.E., 1969. Chapter IV A Roll Tube Method for Cultivation of Strict
508 Anaerobes, in: *Methods in Microbiology*. Elsevier, pp. 117–132.
509 [https://doi.org/10.1016/S0580-9517\(08\)70503-8](https://doi.org/10.1016/S0580-9517(08)70503-8)

510 Kaster, A.-K., Goenrich, M., Seedorf, H., Liesegang, H., Wollherr, A., Gottschalk, G.,
511 Thauer, R.K., 2011. More Than 200 Genes Required for Methane Formation
512 from H₂ and CO₂ and Energy Conservation Are Present in
513 *Methanothermobacter marburgensis* and *Methanothermobacter*
514 *thermautotrophicus*. *Archaea* 2011, 1–23. <https://doi.org/10.1155/2011/973848>

515 Kaul, A., Böllmann, A., Thema, M., Kalb, L., Stöckl, R., Huber, H., Sterner, M.,
516 Bellack, A., 2022. Combining a robust thermophilic methanogen and packing
517 material with high liquid hold-up to optimize biological methanation in trickle-
518 bed reactors. *Bioresour. Technol.* 345, 126524.
519 <https://doi.org/10.1016/j.biortech.2021.126524>

520 Laguillaumie, L., Rafrafi, Y., Moya-Lecalir, E., Delagnes, D., Dubos, S., Spérandio,
521 M., Paul, E., Dumas, C., 2022. Stability of ex situ biological methanation of
522 H₂/CO₂ with a mixed microbial culture in a pilot scale bubble column reactor.
523 *Bioresour. Technol.* 354, 127180.
524 <https://doi.org/10.1016/j.biortech.2022.127180>

525 Lambrecht, J., Cichocki, N., Hübschmann, T., Koch, C., Harms, H., Müller, S., 2017.
526 Flow cytometric quantification, sorting and sequencing of methanogenic archaea

527 based on F420 autofluorescence. *Microb. Cell Factories* 16, 180.
528 <https://doi.org/10.1186/s12934-017-0793-7>

529 Lindsey, R.L., Gladney, L.M., Huang, A.D., Griswold, T., Katz, L.S., Dinsmore, B.A.,
530 Im, M.S., Kucerova, Z., Smith, P.A., Lane, C., Carleton, H.A., 2023. Rapid
531 identification of enteric bacteria from whole genome sequences using average
532 nucleotide identity metrics. *Front. Microbiol.* 14, 1225207.
533 <https://doi.org/10.3389/fmicb.2023.1225207>

534 Liu, T., Li, X., Yekta, S.S., Björn, A., Mu, B.-Z., Masuda, L.S.M., Schnürer, A., Enrich-
535 Prast, A., 2022. Absence of oxygen effect on microbial structure and methane
536 production during drying and rewetting events. *Sci. Rep.* 12, 16570.
537 <https://doi.org/10.1038/s41598-022-20448-5>

538 Lyu, Z., Lu, Y., 2018. Metabolic shift at the class level sheds light on adaptation of
539 methanogens to oxidative environments. *ISME J.* 12, 411–423.
540 <https://doi.org/10.1038/ismej.2017.173>

541 Martin, M., 2011. Cutadapt removes adapter sequences from high-throughput
542 sequencing reads. *EMBnet.journal* 17, 10. <https://doi.org/10.14806/ej.17.1.200>

543 Martin, M.R., Fornero, J.J., Stark, R., Mets, L., Angenent, L.T., 2013. A Single-Culture
544 Bioprocess of *Methanothermobacter thermautotrophicus* to Upgrade Digester
545 Biogas by CO₂-to-CH₄. Conversion with H₂. *Archaea* 2013, 1–11.
546 <https://doi.org/10.1155/2013/157529>

547 Meier-Kolthoff, J.P., Auch, A.F., Klenk, H.-P., Göker, M., 2013. Genome sequence-
548 based species delimitation with confidence intervals and improved distance
549 functions. *BMC Bioinformatics* 14, 60. <https://doi.org/10.1186/1471-2105-14-60>

550 Minh, B.Q., Schmidt, H.A., Chernomor, O., Schrempf, D., Woodhams, M.D., Von
551 Haeseler, A., Lanfear, R., 2020. IQ-TREE 2: New Models and Efficient
552 Methods for Phylogenetic Inference in the Genomic Era. *Mol. Biol. Evol.* 37,
553 1530–1534. <https://doi.org/10.1093/molbev/msaa015>

554 Nakagawa, S., Inagaki, F., Suzuki, Y., Steinsbu, B.O., Lever, M.A., Takai, K., Engelen,
555 B., Sako, Y., Wheat, C.G., Horikoshi, K., Integrated Ocean Drilling Program
556 Expedition 301 Scientists, 2006. Microbial Community in Black Rust Exposed
557 to Hot Ridge Flank Crustal Fluids. *Appl. Environ. Microbiol.* 72, 6789–6799.
558 <https://doi.org/10.1128/AEM.01238-06>

559 Paniagua, S., Lebrero, R., Muñoz, R., 2022. Syngas biomethanation: Current state and
560 future perspectives. *Bioresour. Technol.* 358, 127436.
561 <https://doi.org/10.1016/j.biortech.2022.127436>

562 Pruesse, E., Quast, C., Knittel, K., Fuchs, B.M., Ludwig, W., Peplies, J., Glockner,
563 F.O., 2007. SILVA: a comprehensive online resource for quality checked and
564 aligned ribosomal RNA sequence data compatible with ARB. *Nucleic Acids*
565 *Res.* 35, 7188–7196. <https://doi.org/10.1093/nar/gkm864>

566 Pfeifer, K., Ergal, Í., Koller, M., Basen, M., Schuster, B., Rittmann, S.K.-M.R., 2021.
567 *Archaea Biotechnology*. *Biotechnol. Adv.* 47, 107668.
568 <https://doi.org/10.1016/j.biotechadv.2020.107668>

569 Rachbauer, L., Beyer, R., Bochmann, G., Fuchs, W., 2017. Characteristics of adapted
570 hydrogenotrophic community during biomethanation. *Sci. Total Environ.* 595,
571 912–919. <https://doi.org/10.1016/j.scitotenv.2017.03.074>

572 Rafrafi, Y., Laguillaumie, L., Dumas, C., 2021. Biological Methanation of H₂ and CO₂
573 with Mixed Cultures: Current Advances, Hurdles and Challenges. *Waste*

574 Biomass Valorization 12, 5259–5282. <https://doi.org/10.1007/s12649-020->
575 01283-z

576 Rittmann, S.K.-M.R., Seifert, A.H., Bernacchi, S., 2018. Kinetics, multivariate
577 statistical modelling, and physiology of CO₂-based biological methane
578 production. *Appl. Energy* 216, 751–760.
579 <https://doi.org/10.1016/j.apenergy.2018.01.075>

580 Rognes, T., Flouri, T., Nichols, B., Quince, C., Mahé, F., 2016. VSEARCH: a versatile
581 open source tool for metagenomics. *PeerJ* 4, e2584.
582 <https://doi.org/10.7717/peerj.2584>

583 Seifert, A.H., Rittmann, S., Herwig, C., 2014. Analysis of process related factors to
584 increase volumetric productivity and quality of biomethane with
585 *Methanothermobacter marburgensis*. *Appl. Energy* 132, 155–162.
586 <https://doi.org/10.1016/j.apenergy.2014.07.002>

587 Sun, W., Yu, G., Louie, T., Liu, T., Zhu, C., Xue, G., Gao, P., 2015. From mesophilic to
588 thermophilic digestion: the transitions of anaerobic bacterial, archaeal, and
589 fungal community structures in sludge and manure samples. *Appl. Microbiol.*
590 *Biotechnol.* 99, 10271–10282. <https://doi.org/10.1007/s00253-015-6866-9>

591 Szuhaj, M., Wirth, R., Bagi, Z., Maróti, G., Rákhely, G., Kovács, K.L., 2021.
592 Development of Stable Mixed Microbiota for High Yield Power to Methane
593 Conversion. *Energies* 14, 7336. <https://doi.org/10.3390/en14217336>

594 Tang, Y.Q., Matsui, T., Morimura, S., Wu, X.L., Kida, K., 2008. Effect of Temperature
595 on Microbial Community of a Glucose-Degrading Methanogenic Consortium
596 under Hyperthermophilic Chemostat Cultivation. *J. BioSci. Bioeng.* 106, 180–
597 187. <https://doi.org/10.1263/jbb.106.180>.

598 Thema, M., Weidlich, T., Kaul, A., Böllmann, A., Huber, H., Bellack, A., Karl, J.,
599 Sterner, M., 2021. Optimized biological CO₂-methanation with a pure culture of
600 thermophilic methanogenic archaea in a trickle-bed reactor. *Bioresour. Technol.*
601 333, 125135. <https://doi.org/10.1016/j.biortech.2021.125135>

602 Tong, D., Farnham, D.J., Duan, L., Zhang, Q., Lewis, N.S., Caldeira, K., Davis, S.J.,
603 2021. Geophysical constraints on the reliability of solar and wind power
604 worldwide. *Nat. Commun.* 12, 6146. [https://doi.org/10.1038/s41467-021-26355-](https://doi.org/10.1038/s41467-021-26355-z)
605 [z](https://doi.org/10.1038/s41467-021-26355-z)

606 Treu, L., Kougias, P.G., De Diego-Díaz, B., Campanaro, S., Bassani, I., Fernández-
607 Rodríguez, J., Angelidaki, I., 2018. Two-year microbial adaptation during
608 hydrogen-mediated biogas upgrading process in a serial reactor configuration.
609 *Bioresour. Technol.* 264, 140–147.
610 <https://doi.org/10.1016/j.biortech.2018.05.070>

611 Tsapekos, P., Alvarado-Morales, M., Angelidaki, I., 2022. H₂ competition between
612 homoacetogenic bacteria and methanogenic archaea during biomethantion from
613 a combined experimental-modelling approach. *J. Environ. Chem. Eng.* 10,
614 107281. <https://doi.org/10.1016/j.jece.2022.107281>

615 Vermeij, P., Pennings, J.L., Maassen, S.M., Keltjens, J.T., Vogels, G.D., 1997. Cellular
616 levels of factor 390 and methanogenic enzymes during growth of
617 *Methanobacterium thermoautotrophicum* deltaH. *J. Bacteriol.* 179, 6640–6648.
618 <https://doi.org/10.1128/jb.179.21.6640-6648.1997>

619 Wahid, R., Mulat, D.G., Gaby J.C., Horn, S.V., 2019. Effects of H₂:CO₂ ratio and H₂
620 supply fluctuation on methane content and microbial community composition

621 during *in-situ* biological biogas upgrading. *Biotechnol Biofuels* 12, 104.
622 <https://doi.org/10.1186/s13068-019-1443-6>

623 Wick, R.R., Judd, L.M., Gorrie, C.L., Holt, K.E., 2017. Unicycler: Resolving bacterial
624 genome assemblies from short and long sequencing reads. *PLOS Comput. Biol.*
625 13, e1005595. <https://doi.org/10.1371/journal.pcbi.1005595>

626 Xu, J., Bu, F., Zhu, W., Luo, G., Xie, L., 2020. Microbial Consortiums of
627 Hydrogenotrophic Methanogenic Mixed Cultures in Lab-Scale Ex-Situ Biogas
628 Upgrading Systems under Different Conditions of Temperature, pH and CO.
629 *Microorganisms* 8, 772. <https://doi.org/10.3390/microorganisms8050772>

630
631

632 **Figure captions:**

633 **Figure 1: Relative abundance of microbial taxa inferred from Illumina MiSeq**

634 **sequencing of 16S rRNA genes. (A)** Archaeal abundance at the genus level from the

635 V4-V5 16S rRNA region of the 16S rRNA gene. The pie chart on right indicates

636 abundance of minor genera (<2% of total archaeal reads). **(B)** Bacterial abundance at

637 the phylum level from the V3-V4 16S rRNA region of the 16S rRNA gene. The pie

638 charts on right show the proportion of the different classes and genera constituting the

639 phyla *Bacillota* and *Pseudomonadota*.

640 **Figure 2: Comparative genomics of strain Clermont. (A)** Phylogenomic tree of

641 major archaeal clades based on a 73 genes core set using GToTree v1.8.2. **On left:**

642 Known major clades, including *Methanothermobacter* (dark pink) are collapsed and

643 shown as wedges of different colors. *Halobacteriales* was placed as outgroup. Bar, 0.3

644 substitution per amino acid position. **On right:** Decollapsed *Methanothermobacter*

645 wedge showing the position of strain Clermont (in red) within this genus. Bar, 0.05

646 substitution per amino acid position. **(B)** Collinearity analysis among assemblies of the

647 seven genomes forming the Marburg clade using MUMmer v4.0.0rc1 and visualized

648 using NGenomeSyn. **(C)** Anvi'o representation of the pan-genome of the Marburg

649 clade. Gene clusters (n = 2076) were ordered according to a hierarchical clustering of

650 their presence/absence (inner dendrogram). Rings show the presence (filled) or absence

651 (undashed) of the gene clusters in each genome. Single copy core and other core: gene

652 clusters present in all seven *Methanothermobacter* genomes. Gene clusters exclusively

653 present in a unique genome are indicated by a number: 1. strain K4, 2. strain THM_2, 3.

654 JZ-3_D_bin_25, 4. strain Kepco-1, 5. GMQ_75_MeOH_H2_bin_21, 6. strain Marburg,

655 7. strain Clermont. To the right is given an ANI percentage identity heatmap; red: 100%
656 identity; light red: values ranging from 96% to 97%; white: values <96%.

657 **Figure 3: Methane yield under reduced conditions in batch culture for pure strains**
658 **(i.e. Marburg and Clermont) and the mixed adapted culture.** An asterisk denotes a
659 significant difference ($p < 0.05$) between strain Marburg versus the two other cultures
660 (days 3 to 6), and between the mixed culture versus pure cultures (days 8 and 18). The
661 error bar indicates the standard error (n=3).

662 **Figure 4: Methane yield in batch cultures under oxidative stressed conditions (240**
663 **min of exposure to O₂).** (A) Comparison over time between strain Clermont and mixed
664 adapted culture. (B) Comparison over time between strain Clermont and strain Marburg.
665 An asterisk denotes a significant difference ($p < 0.05$) between cultures over time. The
666 error bar indicates the standard error (n=3).

667 **Figure 5: Schematic representation of oxidative stress protection enzymes detected**
668 **in the Marburg clade genomes.** (A) Gene-loci in the genome of strain Marburg. (B)
669 Potential cellular responses to oxidative stress.

670
671

1 **1 Title**

2
3 **2 Comparison of methane yield of a novel strain of *Methanothermobacter marburgensis***
4
5 **3 in pure and mixed adapted culture derived from a methanation bubble column**
6
7 **4 bioreactor**
8
9

10
11 **5**
12
13 **6 Abstract**

14
15 **7 The ongoing discussion regarding the use of mixed or pure cultures of**
16
17 **8 hydrogenotrophic methanogenic archaea in Power-to-Methane (P2M) bioprocess**
18
19 **9 applications persists, with each option presenting its own advantages and disadvantages.**
20
21 **10 To address this issue, a comparison of methane (CH₄) yield between a novel**
22
23 **11 methanogenic archaeon belonging to the species *Methanothermobacter marburgensis***
24
25 **12 (strain Clermont) isolated from a biological methanation column, and the community**
26
27 **13 from which it originated, was conducted. This comparison included the type strain *M.***
28
29 **14 *marburgensis* str. Marburg. The evaluation also examined how exposure to oxygen (O₂)**
30
31 **15 for up to 240 minutes impacted the CH₄ yield across these cultures. While both**
32
33 **16 *Methanothermobacter* strains exhibit comparable CH₄ yield, slightly higher than that of**
34
35 **17 the mixed adapted culture under non-O₂-exposed conditions, strain Clermont does not**
36
37 **18 display the lag time observed for strain Marburg.**
38
39
40
41
42
43
44
45
46

47 **19**
48 **20 Keywords**

49 **21 *Methanothermobacter marburgensis*, mixed hydrogenotrophic methanogenic culture,**
50
51 **22 oxygen exposure, multi-omics approaches.**
52
53
54

55 **23**
56
57 **24 1. Introduction**
58
59
60
61
62
63
64
65

1 25 To limit the rise of global surface temperature to less than 2°C while meeting the
2
3
4 26 increasing energy demand, a significant global energy transition is urgently needed.
5
6 27 However, shifting away from polluting fossil fuels to low-carbon solutions requires
7
8 28 technological innovation, particularly in renewable energy. Despite substantial progress
9
10 29 in wind, solar, and geothermal energies, challenges such as intermittency, variability,
11
12 30 geographical limitations, and storage persist (Tong et al., 2021). Power-To-Gas (P2G)
13
14 31 concept has emerged as a promising solution allowing the storage of surplus of
15
16 32 renewable energy recovered from the electricity sector in the form of gas (*i.e.*
17
18 33 dihydrogen (H₂) called P2H and CH₄ called P2M) (Glenk and Reichelstein, 2022).
19
20
21
22 34 Currently, P2M offers advantages over P2H. It allows converting electricity into
23
24 35 chemical energy and uses existing infrastructure. Considering storability, it has a higher
25
26 36 energy density (10 kWh/Nm³ for CH₄ versus 3 kWh/Nm³ for H₂) and is suitable for
27
28 37 long term and large-scale storage (Blanco et al., 2018). P2M systems combine H₂
29
30 38 oxidation and carbon dioxide (CO₂) reduction to produce CH₄ using either
31
32 39 physicochemical or biological catalysts (biomethanation). Comparatively,
33
34 40 biomethanation processes require lower temperatures and pressures than
35
36 41 physicochemical methanation processes and exhibit increased resistance to chemical
37
38 42 contaminants including hydrogen sulfide (H₂S), organic acids, or ammonia (Burkhardt
39
40 43 et al., 2015).
41
42 44 Hydrogenotrophic methanogenic archaea (HMs), which can use H₂ as a reducing agent
43
44 45 for the conversion of CO₂ into CH₄, are key biocatalysts for biomethane (Bellini et al.,
45
46 46 2022). They require as much H₂ as the system can provide for CO₂ reduction.
47
48 47 Therefore, the competition and sustainable equilibrium between H₂ producers (*e.g.*
49
50 48 acetogens) and consumers (*e.g.* HMs) usually result in a very low dissolved H₂ partial
51
52
53
54
55
56
57
58
59
60
61
62
63
64
65

1 49 pressure ($p(\text{H}_2)$) to maintain a balanced operation of the entire microbiological
2
3 50 community. However, numerous abiotic and biotic factors can affect this equilibrium.
4
5 51 From a thermodynamical perspective, external H_2 provision strongly favours
6
7 52 hydrogenotrophic methanogenesis. But a sudden increment of $p(\text{H}_2)$ can enable the
8
9 53 homoacetogenic pathway to outcompete the hydrogenotrophic methanogenesis (Treu et
10
11 54 al., 2018; Tsapekos et al., 2022). In addition, temperature, pH, H_2/CO_2 ratio, H_2 supply,
12
13 55 etc, are all abiotic factors that can influence CH_4 content and microbial community
14
15 56 during *in-situ* biological biogas upgrading (Rachbauer et al., 2017; Wahid et al., 2019).
16
17 57 Among HMs, the main actors in biomethanation processes comprise members of the
18
19 58 genera *Methanoculleus*, *Methanothermobacter*, *Methanobacterium*, or *Methanosarcina*.
20
21 59 The relative abundance of these genera in biogas upgrading reactors varies based on
22
23 60 factors such as temperature, pH, carbon monoxide (CO), etc (Thema et al., 2021; Xu et
24
25 61 al., 2020). In thermophilic conditions, *Methanothermobacter* was shown to be
26
27 62 predominant in the mixed cultures due to its favorable growth at higher temperatures
28
29 63 (Kaster et al., 2011; Szuhaj et al., 2021). Within this genus, *Methanothermobacter*
30
31 64 *thermautotrophicus* and *Methanothermobacter marburgensis*, largely used as model
32
33 65 organisms, have already been implemented as biocatalysts in large-scale industrial
34
35 66 processes because they are robust, and reach high cell densities, and CH_4 production
36
37 67 rate (Seifert et al., 2014; Pfeifer et al., 2021; Thema et al., 2021, Kaul et al., 2022).
38
39 68 Two main approaches can be employed for biomethanation, *i.e.* using pure cultures or
40
41 69 enriched mixed cultures, each with its own advantages and drawbacks (Rachbauer et al.,
42
43 70 2017; Rafrafi et al., 2021; Rittmann et al., 2018). Indeed, using single self-replicating
44
45 71 catalysts would prevent oxidation of H_2 by other hydrogenotrophic microorganisms,
46
47 72 thereby avoiding a loss of efficiency in biogas upgrading. It would also allow for better
48
49
50
51
52
53
54
55
56
57
58
59
60
61
62
63
64
65

1 73 system variability and behaviour prediction (Martin et al., 2013). On the other hand,
2
3 74 using consortia would be more efficient, leading to larger CH₄ yields (Bellini et al,
4
5 75 2022, Paniagua et al., 2022). Other advantages of employing consortia include greater
6
7 76 robustness and short recovery time upon starvation/excess input gas rate and
8
9 77 oxygenation. However, managing mixed cultures often requires increased control and a
10
11 78 thorough understanding of how microbial composition impacts the system (Paniagua et
12
13 79 al., 2022). Therefore, despite the growing number of studies in this field, the question of
14
15 80 whether pure or mixed cultures are more suitable for biomethanation processes remains
16
17 81 unresolved. To address this question, a comparison of the performance of both HM pure
18
19 82 cultures and reactor microbiomes from which HMs have been isolated appears essential.
20
21 83 This study aims to evaluate the methanation efficiency of a new HM affiliated to the *M.*
22
23 84 *marburgensis* species (strain Clermont) isolated from a bubble column reactor. Its
24
25 85 methanogenic performance was compared not only with its native consortium but also
26
27 86 with the type strain, *i.e.* *M. marburgensis* strain Marburg (hereinafter referred to as
28
29 87 strain Marburg). This comparison was extended under oxidative stress, a common
30
31 88 occurrence in biomethanation processes.
32
33
34
35
36
37
38
39
40
41

42 90 **2. Material and Methods**

43 91 **2.1. Laboratory-scale methanation reactor**

44 92 The mixed adapted culture used in this study was collected from a 3.5 L bubble column
45
46 93 reactor, six weeks after its inoculation with 300 mL of digestate from a thermophilic
47
48 94 industrial-scale biogas plant treating livestock effluent and agri-food industry wastes
49
50 95 that operates between 52 and 54°C (Methelec, Ennezat, France). Briefly, the reactor
51
52 96 contained 2.7 L of basal anaerobic (BA) culture medium prepared as previously
53
54 97 reported (Bu et al., 2018) and reduced by introducing 0.4 g/L of sodium sulfide
55
56
57
58
59
60
61
62
63
64
65

1 98 nanohydrate ($\text{Na}_2\text{S}\cdot 9\text{H}_2\text{O}$). The H_2/CO_2 gas mixture was set at a ratio of 4:1 (v/v) with a
2
3
4 99 mass flowmeter (SLA5800, Brooks Instrument, Hatfield, USA). Flow rates ranged from
5
6 100 0.29 to 0.44 $\text{NL}\cdot\text{min}^{-1}$. The temperature was set to 55°C using a thermostatic bath (Eco
7
8 101 RE1225 silver, Lauda, Königshofen, Germany).

9
10
11 102 Volatile fatty acids (VFAs) in the six-week mixed adapted culture were determined
12
13 103 using a liquid chromatograph (1260 HPLC, Agilent, Santa Clara, USA). The HPLC
14
15 104 apparatus was equipped with two columns (Rezex ROA 300 x 7.8 nm, Phenomenex,
16
17
18 105 Torrance, USA) mounted in serial in an oven (50°C) and coupled with a refractive index
19
20 106 detector. The mobile phase was a 2 mM sulfuric acid in ultra-pure water pumped at 0.7
21
22 107 $\text{mL}\cdot\text{min}^{-1}$ and 70 bars. For the analysis, 2 mL of sample were mixed with 125 μL of
23
24 108 $\text{Ba}(\text{OH})_2\cdot 8\text{H}_2\text{O}$ (0.3 M) and 125 μL of $\text{ZnSO}_4\cdot 7\text{H}_2\text{O}$ (5% w/v) before a 5 min
25
26 109 centrifugation at 10000 g. Samples were filtered through 0.2 μm nylon filters before
27
28 110 being injected in the HPLC apparatus.

29
30
31 111 Measurements of archaeal and bacterial abundance (quantitative real-time PCR),
32
33 112 performed on the six-week sample mixed adapted culture, revealed a dominance of
34
35 113 archaea over bacteria with an archaea/bacteria ratio of five ($1.0\ 10^9$ archaeal cells/mL
36
37 114 versus $2.2\ 10^8$ bacterial cells/mL).

38 115 **2.2. Microbial community analysis of the mixed adapted culture**

39
40
41 116 Two mL of the six-week mixed adapted culture were centrifuged at 10000 g at room
42
43 117 temperature (RT) for 10 min and total genomic DNA (gDNA) was extracted from the
44
45 118 pellet using a Nucleo Spin Soil kit in accordance with manufacturer's instructions
46
47 119 (Machery Nagel, Düren, Germany). Then, gDNA was quantified using a
48
49 120 spectrophotometer (NanoDrop 1000, Thermo Fisher Scientific, USA). Subsequently,
50
51 121 the V3-V4 hypervariable region of the bacterial 16S ribosomal RNA (rRNA) genes was
52
53
54
55
56
57
58
59
60
61
62
63
64
65

1 122 amplified using the primer set F343 (5'-
2
3 123 CTTTCCCTACACGACGCTCTTCCGATCTACGGRAGGCAGCAG-3') - R784 (5'-
4
5 124 GGAGTTCAGACGTGTGCTCTTCCGATCTTACCAGGGTATCTAATCCT-3')
6
7
8 125 (Carmona-Martinez et al., 2015) while the V4-V5 region of the archaeal 16S rRNA
9
10 126 genes was amplified with the primer set F504-519 (5'-
11
12 127 CTTTCCCTACACGACGCTCTTCCGATCTCAGCMGCCGCGGKAA-3') and R910-
13
14 128 928 (5'-GGAGTTCAGACGTGTGCTCTTCCGATCTCCCGCCWATTCCTTTAAGT-
15
16 129 3') (Braga Nan et al., 2020), primers containing adapters and barcodes for Miseq
17
18 129 3') (Braga Nan et al., 2020), primers containing adapters and barcodes for Miseq
19
20 130 sequencing. PCR reactions contained TaqTM TaKaRa Premix, 1 µM of each primer, 200
21
22 131 µM of each deoxynucleoside triphosphate (dNTP), 0.625 U TaKaRa Taq polymerase
23
24 132 (TakaRa Inc., France), nuclease free-H₂O and 50 to 100 ng gDNA template in a total
25
26 133 volume of 50 µL. For both bacteria and archaea, after a denaturation step of 1 min at
27
28 134 98°C, PCR steps at 98°C for 1 min, 59°C for 40 s, and 72°C for 1 min were repeated 35
29
30 135 times, followed by an elongation step at 72°C for 10 min in a Mastercycler® thermal
31
32 136 cyclor (Eppendorf, Hamburg, Germany). Amplicon size was checked by Agilent High
33
34 137 Sensitivity DNA Kit on 2100 Bioanalyzer (Agilent Technologies, Santa Clara, CA,
35
36 138 USA). Amplicon libraries were prepared and sequenced by the GenoToul platform
37
38 139 (Toulouse, France) with an Illumina MiSeq sequencer to generate 2 x 300 bp paired-end
39
40 140 reads. Bacterial and archaeal reads were separately processed using a homemade
41
42 141 bioinformatics pipeline. Briefly, paired reads were merged using the VSEARCH
43
44 142 v2.18.0 (Rognes et al., 2016) and then trimmed and filtered with Cutadapt (Martin,
45
46 143 2011) to minimize the effects of random sequencing errors as follows: (i) only merged
47
48 144 reads with a length 200-500 bp were kept, (ii) paired reads with sequencing errors in
49
50 145 primers were discarded and (iii) primer sequences and nucleotides with Phred quality
51
52
53
54
55
56
57
58
59
60
61
62
63
64
65

1 146 scores upper than 30 were trimmed. Deletion of chimeric sequences and clusterization
2
3 147 were carried out using VSEARCH (Rognes et al., 2016) and operational taxonomic
4
5 148 units (OTUs) that accounted for <0.005% of the total set of sequences were discarded
6
7
8 149 (Bokulich et al., 2013). The taxonomic assignment was performed against the SILVA
9
10 150 v138.1 SSU NR99 database using the global alignment script in VSEARCH (Pruesse et
11
12
13 151 al, 2007; Rognes et al., 2016).

152 **2.3. Hydrogenotrophic methanogenic archaea isolation and analytical procedures**

153 A serum vial (Dutscher, Bernolsheim, France) containing 50 ml of BA medium (110
19
20 154 mL in capacity) was inoculated with an aliquot of the six-week mixed adapted culture
21
22 155 (10% v/v). After BA medium autoclaving, and prior to its inoculation, dinitrogen (N₂)
23
24 156 filling the head space was replaced by H₂/CO₂ (4:1, v/v) gas mixture from a gas
25
26 157 cylinder (Westfalen, France) at 2 bars. Liquid cultivation was conducted at 55°C in the
27
28 158 dark, without agitation.

31 159 HM isolation was performed *via* successive dilution to extinction series in Hungate
32
33 160 tubes (16.5 mL capacity) containing 5 mL of either liquid or solid BA medium (2% agar
34
35 161 w/v; roll-tube technique (Hungate, 1969)). Headspace composition was determined by
36
37 162 gas chromatography (3000A MicroGC, Agilent Technologies, Santa Clara, CA, USA)
38
39 163 equipped with two capillary columns (one MS-5A column associated with a backflush
40
41 164 injector and one PorapLOT Q column associated with a standard injector) and Soprane
42
43 165 software v3.5.2 for the analysis. The microGC used argon as gas carrier and the
44
45 166 temperature of the columns and injectors were at 50 and 60°C, respectively.

48 167 The purity of HMs was checked by microscopic observations (Leica DM IRB inverted
49
50 168 microscope equipped with a Hamamatsu C13440 camera and Zen Blue v3.1 software)
51
52 169 and by adding yeast extract (2 g/L) and glucose (20 mM final concentration) to the BA
53
54
55
56
57
58
59
60
61
62
63
64
65

1 170 medium to confirm the absence of fermentative bacteria. Subsequently, HM taxonomic
2
3 171 identification was performed by 16S rRNA gene sequence amplification using the
4
5 172 universal primer set Arch21F-1492R (Nakagawa et al., 2006) followed by sequencing
6
7 173 (Eurofins Genomics, Cologne, Germany). For the ultrastructural characterization, the
8
9 174 archaeal cells in 1% (v/v) formaldehyde fixed samples were collected by centrifugation
10
11 175 at 20000 g for 20 min at 14°C directly onto 400-mesh electron microscopy copper grids
12
13 176 covered with carbon-coated Formvar film (AO3X, Pelanne Instruments, Toulouse,
14
15 177 France). Particles were over contrasted with 2% uranyl salts and rinsed three times in
16
17 178 distilled deionized water before being dried at RT. Subsequently, the characterization
18
19 179 was performed with a transmission electron microscope using a JEOL 2100
20
21 180 (Akishikma, Tokyo, Japan; Plateforme CYSTEM, UCA Partner, Clermont-Ferrand,
22
23 181 France). The microscope was operated at 80 kV, and the images were recorded with an
24
25 182 Gatan CMOS RIO 9 camera (Gatan Ametek, Pleasanton, USA) at 3072 x 3072 pixels.
26
27 183 Since all HMs belonged to the same strain, one representative, called
28
29 184 *Methanothermobacter marburgensis* strain Clermont (hereafter referred to as strain
30
31 185 Clermont), was deposited in the Deutsche Sammlung von Mikroorganismen und
32
33 186 Zellkulturen (DSMZ) culture collection (accession number DSM 34405).

187 **2.4. Cultivation procedures**

188 The hydrogenotrophic and methanogenic activities of strain Clermont, the mixed
189 adapted culture, and *M. marburgensis* strain Marburg obtained from DSMZ (DSM
190 2133), which is the closest relative of strain Clermont (99.5% 16S rRNA gene identity),
191 were investigated under reduced conditions. Cultures were conducted in serum vials
192 containing 50 mL of BA medium as described above (Paragraph 2.3). All inoculations
193 were performed with the same number of archaeal cells, *i.e.* 5.7×10^5 cells. Briefly, an

1 194 aliquot of 1 mL of pure or mixed cultures at the end of the exponential growth phase
2
3
4 195 was diluted to 1:10 and directly used for flow cytometry analysis (BD LSR Fortessa X-
5
6 196 20; BD Biosciences, CA, USA). Two lasers (Violet, 405 nm, 50 mW and Blue, 488 nm,
7
8 197 60 mW) were used for F420 cofactor excitation (autofluorescence of archaeal cells) and
9
10 198 morphological characterization, respectively. The threshold was set at 200 on the F420
11
12 199 cofactor parameter. Data were acquired during 60 sec at a constant flow rate of 29.85
13
14 200 $\mu\text{L}/\text{min}$ and processed using FACSDivA 9 software (BD Biosciences).
15
16
17
18 201 Cultures subjected to oxidative stress were inoculated and grown in medium devoid of
19
20 202 chemical reducing agents, namely $\text{Na}_2\text{S}\cdot 9\text{H}_2\text{O}$ and resazurin, generally used to reinforce
21
22 203 anaerobiosis and detect any potential oxidation, to prevent O_2 reduction during the
23
24 204 exposure. Indeed, their presence would have reduced the effective amount of O_2 during
25
26 205 oxic stress. Anaerobiosis prior to oxic stress was confirmed by microGC. After reaching
27
28 206 the end of the exponential growth phase in anaerobic conditions, the cultures were
29
30 207 transferred to sterile beakers in a laminar flow hood and placed under high stirring
31
32 208 speed to be exposed to atmospheric levels of O_2 (21%) for durations of 0, 10, 30, 60, 90,
33
34 209 120, and 240 min. The quantity of dissolved O_2 measured in the medium was $10 \text{ mg}/\text{L} \pm$
35
36 210 $0.32 \text{ mg}/\text{L}$ from 1 min up to 240 min of exposure (portable oximeter, Laqua 200 series,
37
38 211 Horiba Scientific, Japan). Subsequently, fresh BA medium containing a reducing agent
39
40 212 was inoculated as above. The absence of O_2 was checked by gas chromatography before
41
42 213 incubation.
43
44
45
46
47
48 214 All experiments were conducted in biological triplicates. During growth, gas
49
50 215 composition in the headspace was monitored daily by gas chromatography. Statistical
51
52 216 analysis of CH_4 yield during growth was conducted using the Student t-test, one-way or
53
54 217 two-way ANOVA (culture \times incubation days) followed by Tukey's test under normality
55
56
57
58
59
60
61
62
63
64
65

1 218 and homoscedasticity assumption. The level of significance was set at $\alpha=0.05$. All
2
3 219 statistical analyses were performed using the R Stats package v4.2.2.

220 **2.5. DNA extraction for whole genome sequencing of the *M. marburgensis* strain**

221 **Clermont**

222 A culture of strain Clermont (50 mL) in exponential growth was concentrated by
223 centrifugation for 15 min at 10000 g at RT. gDNA was extracted from the pellet using a
224 standard phenol–chloroform method (Biderre-Petit et al, 2024) before quantification on
225 a Qubit Fluorometer (ThermoFisher Scientific, USA) by using QubitTM dsDNA HS
226 assay kit in accordance with manufacturer’s instructions. Subsequently, 300 ng of
227 gDNA were sequenced using Illumina HiSeq technology (2 × 150 bp; Eurofins
228 Genomics, Constance, Germany). Raw paired-end reads were quality-filtered with fastp
229 v0.23.4 (Chen et al., 2018). *De novo* assembly of whole genome sequencing data was
230 performed using Unicycler v0.5.0 (Wick et al., 2017) with default settings. In the
231 following step, the short contigs with viral/transposable elements (BLASTX search
232 against non-redundant database) and fragmented rRNA operons (barrnap v0.9 and
233 parameter "--kingdom arc", <https://github.com/tseemann/barrnap>) were filtered out.

234 **2.6. Phylogenomic tree construction**

235 Representative genomes of *Methanothermobacterium*, *Methanonatronarchaeia*,
236 *Archaeoglobi*, *Methanobacteria*, *Methanococci*, *Methanomicrobia*, *Methanopyri*,
237 *Thermococci*, and *Halobacterium* were downloaded from the National Center for
238 Biotechnology Information (NCBI) RefSeq. Subsequently, a genome-based
239 phylogenetic tree was generated with the program GToTree v1.8.2 as reported in
240 Biderre-Petit et al. (2024), using an archaea-specific gene set composed of 73 markers.
241 Individual gene alignments were concatenated to construct a species tree using IQ-

1 242 TREE v2.2.3 with the evolution model LG+F+I+R10 and parameters "-B 2000 --alrt
2
3 243 2000 --bnni" (Minh et al., 2020). *Halobacterium* was used as an outgroup.
4
5
6 244 **2.7. Pan-genomic analysis and other genome characterizations**
7
8 245 Pan-genomic analysis of the Marburg clade (*i.e.* including the strains Marburg,
9
10 246 Clermont and their closest relatives-strain KEPCO-1 (assembly accession
11
12 247 GCA_008033705.1), strain K4 (GCA_022014235.1), strain THM2
13
14 248 (GCA_009917665.1), bin GMQ_75_MeOH_H2_bin_21 (GCA_030055425.1) and bin
15
16 249 JZ-3_D_bin_25 (GCA_030055435.1); seven genomes in total) was carried out using the
17
18 250 "pan-genomics workflow of anvi'o v7.1 (Delmont and Eren, 2018). The average
19
20 251 nucleotide identity (ANI) was also calculated through anvi'o and to complete the
21
22 252 results, *in silico* DNA-DNA hybridization (*isDDH*) was computed using Genome-to-
23
24 253 Genome Distance Calculator v2.1 with formula 2 as previously recommended (Meier-
25
26 254 Kolthoff et al., 2013). Genome synteny was visualized by NGenomeSyn v1.41 (He et
27
28 255 al., 2023).

256 257 **3. Results and discussion**

258 **3.1. Overview of microbial community diversity in a bubble column reactor**

259 Metabarcoding procedure was used to separately address the archaeal and bacterial
260 diversity present in the six-week adapted culture. Although less abundant than archaea,
261 bacteria showed much higher diversity, with 833 OTUs (19403 reads in total) versus 42
262 OTUs (28482 reads), respectively, which is consistent with what is generally described
263 for mixed cultures (Xu et al., 2020). For the archaea, the four most abundant OTUs
264 (>1% relative abundance in the sample) covered 96.1% of the community (See
265 supplementary material). *Methanothermobacter* genus represented 98.5% of the

1 266 archaeal community in terms of reads, followed by *Methanobacterium* (1.2%),
2
3 267 *Methanomassiliicoccus* (0.09%) and *Methanoculleus* (0.01%) (Fig. 1A). This finding
4
5 268 closely aligns with previous research, which has shown that *Methanothermobacter* is
6
7
8 269 the dominant genus in the hydrogenotrophic methanogenic consortium of *ex-situ*
9
10 270 methanation systems at 55°C (Xu et al., 2020). Within this genus, 98.9% of the reads
11
12 271 are affiliated to the *M. marburgensis* species (>97% 16S rRNA gene sequence identity).
13
14 272 Regarding bacteria, the most represented phyla in terms of reads were *Bacillota* (ex
15
16 273 *Firmicutes*, 91.8% of total bacterial reads) followed by *Pseudomonadota* (ex
17
18 274 *Proteobacteria*, 6.8%) (Fig. 1B), in agreement with previous studies (Bassani et al.,
19
20 275 2015; Campanaro et al., 2020). The 11 most abundant OTUs (>1% relative abundance
21
22 276 in the sample) covered 48.7% of the bacterial community (See supplementary material)
23
24 277 and mostly affiliated with the genus *Haloplasma* (35.2% of all bacterial reads) and the
25
26 278 class *Limnochordia* (33.2%) in *Bacillota*.
27
28 279 The most abundant taxon, *i.e.* *Haloplasma*, is currently represented by only one
29
30 280 representative, a halophilic bacterium isolated from a deep-sea brine lake, named *H.*
31
32 281 *contractile*. The growth limit of this bacterium was determined at 44°C (Antunes et al,
33
34 282 2008), which is not in accordance with the temperature used in this study, *i.e.* 55°C.
35
36 283 However, although SILVA classifies this predominant taxon in the genus *Haloplasma*,
37
38 284 the sequence used as reference and which shows 99% identity with OTUs affiliated to
39
40 285 *Haloplasma* (accession number FN436037, see supplementary material), displays only
41
42 286 up to 89% sequence similarity with *Haloplasma* using BLAST N against the nucleotide
43
44 287 database in NCBI. This may be due to the low number of sequences representative of
45
46 288 the genus *Haloplasma* and also more generally of the family and order. Indeed, the
47
48 289 order Haloplasmatales currently includes a single family -Haloplasmataceae- which
49
50
51
52
53
54
55
56
57
58
59
60
61
62
63
64
65

1 290 includes a single genus and species: *H. contractile*. This most likely not only leads to an
2
3
4 291 inaccurate affiliation at the genus level, but also potentially at the family level.
5
6 292 Consequently, the representatives that will be discovered for this group of
7
8 293 Haloplasmatales will most certainly allow significant changes to the current description
9
10 294 made for the single type species.
11
12 295 The second most abundant taxon, the *Limnochordia* class, is frequently observed in full-
13
14
15 296 size and laboratory-scale thermophilic biogas reactors (Campanaro et al., 2020). The
16
17 297 main representative in this class was MBA03 (14.6% of all bacterial reads).
18
19 298 Laguillaumie et al. (2022) suggested that MBA03, referenced as a carbohydrate
20
21 299 fermentative taxon, would grow on lysis products and prevent side products, such as
22
23 300 VFAs, from accumulating in the reactor. The low amount of VFAs measured in the
24
25 301 reactor could therefore be explained, at least in part, by the MBA03 abundance. This
26
27 302 low quantity also indicates that hydrogenotrophic methanogenesis has not shifted
28
29 303 towards homoacetogenesis. Moreover, MBA03 association with *Methanobacterium* was
30
31 304 described as an indicator of process stability (Laguillaumie et al., 2022). Its association
32
33 305 with *Methanothermobacter* could therefore still be such an indicator.
34
35 306 In addition to MBA03, two other bacteria known to be syntrophic acetate oxidizing, *i.e.*
36
37 307 *Tepidiphilus (Pseudomonadota)* and norank order D8A-2 (*Bacillota*), showed
38
39 308 significant relative abundance, with 2.9% and 3.6% of all bacterial reads, respectively.
40
41 309 These results are in line with previous studies, which showed that these taxa were
42
43 310 abundant in thermophilic samples and worked synergistically with HMs, providing the
44
45 311 substrates they need towards biogas production (Tang et al., 2008; Xu et al., 2020). An
46
47 312 anaerobic digestion system seeded from manure samples (which is comparable to what
48
49 313 was used for the bioreactor, *i.e.* a biogas plant treating livestock effluent) and running at
50
51
52
53
54
55
56
57
58
59
60
61
62
63
64
65

1 314 55°C (Sun et al., 2015), was shown to be populated with similar microbial taxa. This
2
3 315 supports the view that temperature, but also inoculum, are crucial variables in
4
5 316 determining the structure of microbial consortia in hydrogenotrophic methanogenic
6
7 317 mixed cultures (Xu et al., 2020).
8
9

10 318 **3.2. Isolation and genome sequencing of *M. marburgensis* strain Clermont**

11 319 The strain isolated from the bioreactor belonged to the genus *Methanothermobacter* and
12
13 320 showed >99.5% identity with strain Marburg 16S rRNA gene sequence (accession
14
15 321 number NR_102881.1). It was named *M. marburgensis* strain Clermont and deposited
16
17 322 in the DSMZ collection (DSM 34405). This strain was rod-shaped (~5 µm long and 0.6
18
19 323 µm wide) and non-motile (See supplementary material).
20
21
22

23 324 The draft genome of strain Clermont (~330-fold coverage), featuring six contigs (from
24
25 325 ~21.9 to 776.9 kb), had a total length of ~1.72 Mb, a N50 contig length of 593 kb, and
26
27 326 a G+C content of 48.7%. The number of coding DNA sequences was 1805 with two
28
29 327 16S-23S rRNA gene clusters, three 5S rRNA genes and 37 transfer RNA (tRNA) genes.
30
31 328 No extra-chromosomal genetic elements were detected. Genome fragmentation was
32
33 329 mainly due to the high conservation degree between rRNA operons and transposase
34
35 330 sequences that hamper the assembly tool to resolve these loci. Phylogenomic analysis
36
37 331 confirmed the close relationship of strain Clermont with strain Marburg but also with
38
39 332 three other *Methanothermobacter* strains (*i.e.* KEPCO-1, THM_2, and K4) and two bins
40
41 333 (*i.e.* GMQ_75_MeOH_H2_bin_21 and JZ-3_D_bin_25). They all formed a clade
42
43 334 (hereinafter referred to as Marburg clade) within the genus *Methanothermobacter* (Fig.
44
45 335 2A). Their genomes revealed a high degree of synteny (Fig. 2B). Based on ANI and
46
47 336 *is*DDH values, strains Clermont, Marburg, KEPCO_1 and THM_2 formed a single
48
49 337 species (ANI ≥96% and DDH ~70%; thresholds proposed for species definition
50
51
52
53
54
55
56
57
58
59
60
61
62
63
64
65

1 338 (Lindsey et al., 2023)) while strain K4 and the bins represented three novel
2
3 339 *Methanothermobacter* species (Fig. 2C).
4
5 340 At the pan-genome level, the Marburg clade comprised 2076 gene clusters (GCs) with
6
7 341 1564 (75.3%) forming the core genome (shared by all seven genomes), 324 (15.6%)
8
9 342 constituting the accessory genome (specific to a subset of genomes) and 188 (9.1%)
10
11 343 being unique to a single genome (Fig. 2C). The core genome contained the full suite for
12
13 344 proteins encoded to carry out the hydrogenotrophic pathway. Members of this clade can
14
15 345 assimilate acetyl-coA *via* the CO-methylating acetyl-CoA synthase from methyl-
16
17 346 tetrahydromethanopterin. In strain Marburg, this complex was also shown to play a key
18
19 347 role in CO oxidation (Diender et al., 2016). Moreover, the presence of all genes
20
21 348 involved in carboxydrotrophic methanogenesis in all Marburg clade genomes suggests
22
23 349 they are also able to grow with CO as the sole carbon source. A protein of the carbonic
24
25 350 anhydrase family (Cah), known to potentially convert bicarbonate into bioavailable
26
27 351 CO₂, was also present. Finally, as strains Clermont and Marburg were unable to grow
28
29 352 on formate as an energy source (data not shown), the function of the formate
30
31 353 dehydrogenase (FdhAB) is likely to reduce CO₂ to formate for its use in the purine
32
33 354 synthesis (Kaster et al, 2011).
34
35

355 **3.3. Comparison of CH₄ yields between the pure cultures-strains Clermont and** 36 **Marburg-, and the mixed adapted culture**

357 ***3.3.1. CH₄ yield during growth under reduced conditions***

358 The isolation of a new strain for the species *M. marburgensis* (strain Clermont) from a
359 reactor microbiome enabled to compare CH₄ yield not only between two strains of the
360 same species but also between strain Clermont and the community from which it was
361 isolated. In this respect, a flow cytometry method based on the cofactor F420

1 362 fluorescence (Lambrecht et al., 2017) was used for quantification and each culture was
2
3 363 inoculated with 5.7×10^5 archaeal cells. The maximum specific growth rates (μ_{MAX})
4
5 364 were 0.017, 0.03 and 0.02 h^{-1} for strain Clermont, Marburg and the mixed adapted
6
7
8 365 culture, respectively.
9
10 366 Methanogenic activity was observed at one-day post-inoculation for strain Clermont
11
12 367 and the mixed adapted culture (Fig. 3). CH_4 yield increased linearly until total H_2
13
14 368 conversion, reaching a maximum value after six days of growth, corresponding to
15
16 369 $54.3\% \pm 1.4\%$ CH_4 in the gas fraction for strain Clermont and to $49.3\% \pm 2.6\%$ for the
17
18 370 mixed adapted culture ($p < 0.05$). This aligns with the view that the use of unique, self-
19
20 371 replicating catalysts would avoid a loss of efficiency in biogas upgrading due to H_2
21
22 372 oxidation by other hydrogenotrophic microorganisms (Martin et al, 2013).
23
24 373 For strain Marburg, methanogenic activity was observed three days post-inoculation,
25
26 374 *i.e.* with a two-day lag phase compared with strain Clermont. Total H_2 conversion was
27
28 375 observed after eight days of growth, resulting in a maximum of $53.9\% \pm 2.4\%$ CH_4 in
29
30 376 the gas fraction, a proportion similar to that obtained for strain Clermont (Fig. 3,
31
32 377 $p > 0.05$). Consequently, the medium used in this study (*i.e.* BA medium), which is that
33
34 378 used for the isolation of strain Clermont, favoured the growth behaviour of the latter but
35
36 379 not its CH_4 yield. As the two pure strains are genetically very close, one explanation of
37
38 380 the two-day delay for strain Marburg may be, in part, attributed to their accessory
39
40 381 genomes. Indeed, the genome of strain Clermont contains 121 genes that are not present
41
42 382 in strain Marburg while the genome of strain Marburg contains 49 genes not found in
43
44 383 strain Clermont, all mostly organized into clusters (the largest contained 34 genes for
45
46 384 strain Clermont while 11 genes, for strain Marburg; See supplementary material).
47
48 385 Among these accessory genes, those encoding glycosyltransferases associated with the
49
50
51
52
53
54
55
56
57
58
59
60
61
62
63
64
65

1 386 synthesis and glycosylation of cellular surface proteins (*e.g* RafB, WcaA, WcaE) were
2
3 387 more abundant in strain Clermont (See supplementary material). Kaster et al. (2011)
4
5 388 suggested that these protein families might be partially responsible for the observed
6
7 389 differences in growth rate phenotype between strain Marburg and *M.*
8
9
10 390 *thermautotrophicus*. If this hypothesis proves to be true, it could also partly account for
11
12 391 the observed phenotypic differences between strains Clermont and Marburg.
13
14

15 392 **3.3.2. CH₄ yield following oxidative stress**

16
17
18 393 As methanation reactors can experience episodic oxygenation (accidents, maintenance
19
20 394 operations), it is essential to assess the HMs ability to maintain CH₄ yield after exposure
21
22 395 to O₂. This has never been done for *Methanothermobacter* species, either in pure or
23
24 396 mixed cultures. Interestingly, the results showed that O₂ exposure had no impact on the
25
26 397 pure strains (*i.e.* strains Clermont and Marburg) as they exhibited the same CH₄ yield
27
28 398 levels when all H₂ was consumed (*e.g.* 51.2% ± 1.6% and 55.3% ± 2.3%, respectively;
29
30 399 after 240 min of O₂ exposure, Fig. 4B), whatever the time of exposure to O₂, *i.e* from 0
31
32 400 min up to 240 min (p>0.05; See supplemental material). The O₂ resistance capacity of
33
34 401 these strains is suspected to be mediated by the presence in their genome of energy-free
35
36 402 reactive oxygen species (ROS) scavengers of various protection enzymes, *i.e.*
37
38 403 superoxide dismutase (SOD), superoxide reductase (SOR), F₄₂₀H₂₀ oxidase (FprA),
39
40 404 peroxiredoxin (PRX), and rubrerythrin (Rbr) (Fig. 5), as previously reported for other
41
42 405 methanogens (Liu et al., 2022). However, no catalase-encoding gene was found, similar
43
44 406 to what was observed by Lyu and Lu (2018) in the Class I methanogens (*i.e.*
45
46 407 *Methanobacteriales*, *Methanocellales* and *Methanopyrales*) to which
47
48 408 *Methanothermobacter* spp. belongs. In all Marburg clade genomes, most ROS
49
50 409 scavengers co-localize with genes encoding protection enzymes like rubredoxin (Rub,
51
52
53
54
55
56
57
58
59
60
61
62
63
64
65

1 410 electron providers to SOD and SOR), ferritin (FtnA, iron detoxifier during transient O₂)
2
3 411 (Fig. 5) and F390-synthetase which is thought to have a regulatory function in O₂ stress
4
5 412 response (Vermeij et al., 1997). As most of these genes are up-regulated during the
6
7 413 growth of strain Marburg on CO, it was hypothesized that they respond to redox stress
8
9 414 in general, and not just to O₂ stress, or are regulated by universal stress proteins
10
11 415 (Diender et al., 2016). Moreover, strain Marburg still shows the same two-day lag
12
13 416 compared with strain Clermont. Its growth behaviour is therefore not altered by oxic
14
15 417 stress either.

16
17
18 418 Conversely, exposure to O₂ has an impact on CH₄ yield by the mixed adapted culture.
19
20 419 Indeed, it exhibited a slight increase from the sixth day of incubation, when all H₂ was
21
22 420 converted, with 50.1% ± 1.6% CH₄ yield at 240 min of O₂ exposure (Fig. 4A) versus
23
24 421 46.4% ± 2.9% at 0 min (p<0.02; See supplementary material), thereby reaching the
25
26 422 level of the pure cultures (Fig. 4B). This gap in CH₄ yield could be associated with the
27
28 423 inhibition of hydrogenotrophic microorganisms, other than strain Clermont, present in
29
30 424 the mixed adapted culture.
31
32
33
34
35
36

37 425

38 426 **4. Conclusions**

39
40 427 Although methanogenesis is well studied, gaps remain in the understanding of
41
42 428 biometanation, particularly regarding the choice between pure and mixed cultures in an
43
44 429 energy bioprocess. Comparative analysis of bioenergetic performances between strain
45
46 430 Clermont and its native consortium shows that the pure strain outperforms the
47
48 431 consortium in CH₄ yield under reduced conditions. However, this is no longer the case
49
50 432 after exposure to O₂. Furthermore, although both pure strains show the same CH₄ yield,
51
52
53
54
55
56
57
58
59
60
61
62
63
64
65

1 433 strain Clermont displays a higher reaction speed than the type strain of its species under
2
3 434 the culture conditions used in this study.

4
5
6 435

7
8 436 E-supplementary data of this work can be found in online version of the paper.

9
10
11 437

12 438 **Data availability**

13
14
15 439 The raw reads of the 16S rRNA gene sequencing and genomic data were deposited at

16
17
18 440 the NCBI database under the BioProject PRJNA1044399. *M. marburgensis* strain

19
20
21 441 Clermont was deposited in the DSMZ German Collection of Microorganisms under

22
23 442 accession number DSM 34405. Although the strain is not in the DSMZ catalogue or

24
25 443 website, it is available on demand.

26
27
28 444

29 445 **References**

30
31
32 446 Antunes, A, Rainey, F.A., Wanner, G., Taborda, M., Pätzold, J., Nobre, M.F., da Costa,

33
34
35 447 M.S., Huber, R., 2008. A new lineage of halophilic, wall-less, contractile

36
37 448 bacteria from a brine-filled deep of the Red Sea. *J. Bacteriol.* 190, 3580-3587.

38
39
40 449 [https://doi.org/ 10.1128/JB.01860-07](https://doi.org/10.1128/JB.01860-07)

41
42 450 Bassani, I., Kougias, P.G., Treu, L., Angelidaki, I., 2015. Biogas Upgrading via

43
44 451 Hydrogenotrophic Methanogenesis in Two-Stage Continuous Stirred Tank

45
46 452 Reactors at Mesophilic and Thermophilic Conditions. *Environ. Sci. Technol.* 49,

47
48
49 453 12585–12593. <https://doi.org/10.1021/acs.est.5b03451>

50
51
52 454 Bellini, R., Bassani, I., Vizzarro, A., Azim, A., Vasile, N., Pirri, C., Verga, F., Menin,

53
54
55 455 B., 2022. Biological Aspects, Advancements and Techno-Economical

56
57
58
59
60
61
62
63
64
65

1 456 Evaluation of Biological Methanation for the Recycling and Valorization of
2
3 457 CO₂. *Energies* 15, 4064. <https://doi.org/10.3390/en15114064>
4
5
6 458 Biderre-Petit, C., Courtine, D., Hennequin, C., Galand, P.E., Bertilsson, S., Debroas, D.,
7
8 459 Monjot, A., Lepère, C., Divne, A., Hochart, C., 2024. A pan-genomic approach
9
10 460 reveals novel *Sulfurimonas* clade in the ferruginous meromictic Lake Pavin.
11
12 461 *Mol. Ecol. Resour.* e13923. <https://doi.org/10.1111/1755-0998.13923>
13
14
15 462 Blanco, H., Nijs, W., Ruf, J., Faaij, A., 2018. Potential of Power-to-Methane in the EU
16
17 463 energy transition to a low carbon system using cost optimization. *Appl. Energy*
18
19 464 232, 323–340. <https://doi.org/10.1016/j.apenergy.2018.08.027>
20
21
22 465 Bokulich, N.A., Subramanian, S., Faith, J.J., Gevers, D., Gordon, J.I., Knight, R., Mills,
23
24 466 D.A., Caporaso, J.G., 2013. Quality-filtering vastly improves diversity estimates
25
26 467 from Illumina amplicon sequencing. *Nat. Methods* 10, 57–59.
27
28 468 <https://doi.org/10.1038/nmeth.2276>
29
30
31 469 Braga Nan, L., Trably, E., Santa-Catalina, G., Bernet, N., Delgenès, J.-P., Escudié, R.,
32
33 470 2020. Biomethanation processes: new insights on the effect of a high H₂ partial
34
35 471 pressure on microbial communities. *Biotechnol. Biofuels* 13, 141.
36
37 472 <https://doi.org/10.1186/s13068-020-01776-y>
38
39
40 473 Bu, F., Dong, N., Kumar Khanal, S., Xie, L., Zhou, Q., 2018. Effects of CO on
41
42 474 hydrogenotrophic methanogenesis under thermophilic and extreme-thermophilic
43
44 475 conditions: Microbial community and biomethanation pathways. *Bioresour.*
45
46 476 *Technol.* 266, 364–373. <https://doi.org/10.1016/j.biortech.2018.03.092>
47
48
49 477 Burkhardt, M., Koschack, T., Busch, G., 2015. Biocatalytic methanation of hydrogen
50
51 478 and carbon dioxide in an anaerobic three-phase system. *Bioresour. Technol.* 178,
52
53 479 330–333. <https://doi.org/10.1016/j.biortech.2014.08.023>
54
55
56
57
58
59
60
61
62
63
64
65

1 480 Campanaro, S., Treu, L., Rodriguez-R, L.M., Kovalovszki, A., Ziels, R.M., Maus, I.,
2
3
4 481 Zhu, X., Kougias, P.G., Basile, A., Luo, G., Schlüter, A., Konstantinidis, K.T.,
5
6 482 Angelidaki, I., 2020. New insights from the biogas microbiome by
7
8 483 comprehensive genome-resolved metagenomics of nearly 1600 species
9
10
11 484 originating from multiple anaerobic digesters. *Biotechnol. Biofuels* 13, 25.
12
13 485 <https://doi.org/10.1186/s13068-020-01679-y>
14
15
16 486 Carmona-Martínez, A.A., Trably, E., Milferstedt, K., Lacroix, R., Etcheverry, L.,
17
18 487 Bernet, N., 2015. Long-term continuous production of H₂ in a microbial
19
20 488 electrolysis cell (MEC) treating saline wastewater. *Water Res.* 81, 149–156.
21
22 489 <https://doi.org/10.1016/j.watres.2015.05.041>
23
24
25
26 490 Chen, S., Zhou, Y., Chen, Y., Gu, J., 2018. fastp: an ultra-fast all-in-one FASTQ
27
28 491 preprocessor. *Bioinformatics* 34, i884–i890.
29
30 492 <https://doi.org/10.1093/bioinformatics/bty560>
31
32
33 493 Delmont, T.O., Eren, A.M., 2018. Linking pangenomes and metagenomes: the
34
35 494 *Prochlorococcus* metapangenome. *PeerJ.* 6, e4320.
36
37 495 <https://doi.org/10.7717/peerj.4320>
38
39
40
41 496 Diender, M., Pereira, R., Wessels, H.J.C.T., Stams, A.J.M., Sousa, D.Z., 2016.
42
43 497 Proteomic Analysis of the Hydrogen and Carbon Monoxide Metabolism of
44
45 498 *Methanothermobacter marburgensis*. *Front. Microbiol.* 7.
46
47 499 <https://doi.org/10.3389/fmicb.2016.01049>
48
49
50
51 500 Glenk, G., Reichelstein, S., 2022. Reversible Power-to-Gas systems for energy
52
53 501 conversion and storage. *Nat. Commun.* 13, 2010.
54
55 502 <https://doi.org/10.1038/s41467-022-29520-0>
56
57
58
59
60
61
62
63
64
65

1 503 He, W., Yang, J., Jing, Y., Xu, L., Yu, K., Fang, X., 2023. NGenomeSyn: an easy-to-
2
3 504 use and flexible tool for publication-ready visualization of syntenic relationships
4
5 505 across multiple genomes. *Bioinformatics* 39, btad121.
6
7 506 <https://doi.org/10.1093/bioinformatics/btad121>
8
9
10 507 Hungate, R.E., 1969. Chapter IV A Roll Tube Method for Cultivation of Strict
11
12 508 Anaerobes, in: *Methods in Microbiology*. Elsevier, pp. 117–132.
13
14 509 [https://doi.org/10.1016/S0580-9517\(08\)70503-8](https://doi.org/10.1016/S0580-9517(08)70503-8)
15
16
17 510 Kaster, A.-K., Goenrich, M., Seedorf, H., Liesegang, H., Wollherr, A., Gottschalk, G.,
18
19 511 Thauer, R.K., 2011. More Than 200 Genes Required for Methane Formation
20
21 512 from H₂ and CO₂ and Energy Conservation Are Present in
22
23 513 *Methanothermobacter marburgensis* and *Methanothermobacter*
24
25 514 *thermautotrophicus*. *Archaea* 2011, 1–23. <https://doi.org/10.1155/2011/973848>
26
27
28
29 515 Kaul, A., Böllmann, A., Thema, M., Kalb, L., Stöckl, R., Huber, H., Sterner, M.,
30
31 516 Bellack, A., 2022. Combining a robust thermophilic methanogen and packing
32
33 517 material with high liquid hold-up to optimize biological methanation in trickle-
34
35 518 bed reactors. *Bioresour. Technol.* 345, 126524.
36
37 519 <https://doi.org/10.1016/j.biortech.2021.126524>
38
39
40
41 520 Laguillaumie, L., Rafrafi, Y., Moya-Lecalir, E., Delagnes, D., Dubos, S., Spérandio,
42
43 521 M., Paul, E., Dumas, C., 2022. Stability of ex situ biological methanation of
44
45 522 H₂/CO₂ with a mixed microbial culture in a pilot scale bubble column reactor.
46
47 523 *Bioresour. Technol.* 354, 127180.
48
49 524 <https://doi.org/10.1016/j.biortech.2022.127180>
50
51
52
53 525 Lambrecht, J., Cichocki, N., Hübschmann, T., Koch, C., Harms, H., Müller, S., 2017.
54
55 526 Flow cytometric quantification, sorting and sequencing of methanogenic archaea
56
57
58
59
60
61
62
63
64
65

1 527 based on F420 autofluorescence. *Microb. Cell Factories* 16, 180.
2
3 528 <https://doi.org/10.1186/s12934-017-0793-7>
4
5 529 Lindsey, R.L., Gladney, L.M., Huang, A.D., Griswold, T., Katz, L.S., Dinsmore, B.A.,
6
7
8 530 Im, M.S., Kucerova, Z., Smith, P.A., Lane, C., Carleton, H.A., 2023. Rapid
9
10 531 identification of enteric bacteria from whole genome sequences using average
11
12 532 nucleotide identity metrics. *Front. Microbiol.* 14, 1225207.
13
14 533 <https://doi.org/10.3389/fmicb.2023.1225207>
15
16 534 Liu, T., Li, X., Yekta, S.S., Björn, A., Mu, B.-Z., Masuda, L.S.M., Schnürer, A., Enrich-
17
18 535 Prast, A., 2022. Absence of oxygen effect on microbial structure and methane
19
20 536 production during drying and rewetting events. *Sci. Rep.* 12, 16570.
21
22 537 <https://doi.org/10.1038/s41598-022-20448-5>
23
24 538 Lyu, Z., Lu, Y., 2018. Metabolic shift at the class level sheds light on adaptation of
25
26 539 methanogens to oxidative environments. *ISME J.* 12, 411–423.
27
28 540 <https://doi.org/10.1038/ismej.2017.173>
29
30 541 Martin, M., 2011. Cutadapt removes adapter sequences from high-throughput
31
32 542 sequencing reads. *EMBnet.journal* 17, 10. <https://doi.org/10.14806/ej.17.1.200>
33
34 543 Martin, M.R., Fornero, J.J., Stark, R., Mets, L., Angenent, L.T., 2013. A Single-Culture
35
36 544 Bioprocess of *Methanothermobacter thermautotrophicus* to Upgrade Digester
37
38 545 Biogas by CO₂-to-CH₄. Conversion with H₂. *Archaea* 2013, 1–11.
39
40 546 <https://doi.org/10.1155/2013/157529>
41
42 547 Meier-Kolthoff, J.P., Auch, A.F., Klenk, H.-P., Göker, M., 2013. Genome sequence-
43
44 548 based species delimitation with confidence intervals and improved distance
45
46 549 functions. *BMC Bioinformatics* 14, 60. <https://doi.org/10.1186/1471-2105-14-60>
47
48
49
50
51
52
53
54
55
56
57
58
59
60
61
62
63
64
65

1 550 Minh, B.Q., Schmidt, H.A., Chernomor, O., Schrempf, D., Woodhams, M.D., Von
2
3 551 Haeseler, A., Lanfear, R., 2020. IQ-TREE 2: New Models and Efficient
4
5 552 Methods for Phylogenetic Inference in the Genomic Era. *Mol. Biol. Evol.* 37,
6
7 553 1530–1534. <https://doi.org/10.1093/molbev/msaa015>
8
9
10 554 Nakagawa, S., Inagaki, F., Suzuki, Y., Steinsbu, B.O., Lever, M.A., Takai, K., Engelen,
11
12 555 B., Sako, Y., Wheat, C.G., Horikoshi, K., Integrated Ocean Drilling Program
13
14 556 Expedition 301 Scientists, 2006. Microbial Community in Black Rust Exposed
15
16 557 to Hot Ridge Flank Crustal Fluids. *Appl. Environ. Microbiol.* 72, 6789–6799.
17
18 558 <https://doi.org/10.1128/AEM.01238-06>
19
20
21 559 Paniagua, S., Lebrero, R., Muñoz, R., 2022. Syngas biomethanation: Current state and
22
23 560 future perspectives. *Bioresour. Technol.* 358, 127436.
24
25 561 <https://doi.org/10.1016/j.biortech.2022.127436>
26
27
28 562 Pruesse, E., Quast, C., Knittel, K., Fuchs, B.M., Ludwig, W., Peplies, J., Glockner,
29
30 563 F.O., 2007. SILVA: a comprehensive online resource for quality checked and
31
32 564 aligned ribosomal RNA sequence data compatible with ARB. *Nucleic Acids*
33
34 565 *Res.* 35, 7188–7196. <https://doi.org/10.1093/nar/gkm864>
35
36
37 566 Pfeifer, K., Ergal, Í., Koller, M., Basen, M., Schuster, B., Rittmann, S.K.-M.R., 2021.
38
39 567 *Archaea Biotechnology. Biotechnol. Adv.* 47, 107668.
40
41 568 <https://doi.org/10.1016/j.biotechadv.2020.107668>
42
43
44 569 Rachbauer, L., Beyer, R., Bochmann, G., Fuchs, W., 2017. Characteristics of adapted
45
46 570 hydrogenotrophic community during biomethanation. *Sci. Total Environ.* 595,
47
48 571 912–919. <https://doi.org/10.1016/j.scitotenv.2017.03.074>
49
50
51 572 Rafrafi, Y., Laguillaumie, L., Dumas, C., 2021. Biological Methanation of H₂ and CO₂
52
53 573 with Mixed Cultures: Current Advances, Hurdles and Challenges. *Waste*
54
55
56
57
58
59
60
61
62
63
64
65

1 574 Biomass Valorization 12, 5259–5282. <https://doi.org/10.1007/s12649-020->
2
3 575 01283-z
4
5
6 576 Rittmann, S.K.-M.R., Seifert, A.H., Bernacchi, S., 2018. Kinetics, multivariate
7
8 577 statistical modelling, and physiology of CO₂-based biological methane
9
10 578 production. *Appl. Energy* 216, 751–760.
11
12 579 <https://doi.org/10.1016/j.apenergy.2018.01.075>
13
14
15 580 Rognes, T., Flouri, T., Nichols, B., Quince, C., Mahé, F., 2016. VSEARCH: a versatile
16
17 581 open source tool for metagenomics. *PeerJ* 4, e2584.
18
19 582 <https://doi.org/10.7717/peerj.2584>
20
21
22 583 Seifert, A.H., Rittmann, S., Herwig, C., 2014. Analysis of process related factors to
23
24 584 increase volumetric productivity and quality of biomethane with
25
26 585 *Methanothermobacter marburgensis*. *Appl. Energy* 132, 155–162.
27
28 586 <https://doi.org/10.1016/j.apenergy.2014.07.002>
29
30
31 587 Sun, W., Yu, G., Louie, T., Liu, T., Zhu, C., Xue, G., Gao, P., 2015. From mesophilic to
32
33 588 thermophilic digestion: the transitions of anaerobic bacterial, archaeal, and
34
35 589 fungal community structures in sludge and manure samples. *Appl. Microbiol.*
36
37 590 *Biotechnol.* 99, 10271–10282. <https://doi.org/10.1007/s00253-015-6866-9>
38
39
40 591 Szuhaj, M., Wirth, R., Bagi, Z., Maróti, G., Rákhely, G., Kovács, K.L., 2021.
41
42 592 Development of Stable Mixed Microbiota for High Yield Power to Methane
43
44 593 Conversion. *Energies* 14, 7336. <https://doi.org/10.3390/en14217336>
45
46
47 594 Tang, Y.Q., Matsui, T., Morimura, S., Wu, X.L., Kida, K., 2008. Effect of Temperature
48
49 595 on Microbial Community of a Glucose-Degrading Methanogenic Consortium
50
51 596 under Hyperthermophilic Chemostat Cultivation. *J. BioSci. Bioeng.* 106, 180–
52
53 597 187. <https://doi.org/10.1263/jbb.106.180>.
54
55
56
57
58
59
60
61
62
63
64
65

- 1 598 Thema, M., Weidlich, T., Kaul, A., Böllmann, A., Huber, H., Bellack, A., Karl, J.,
2
3 599 Sterner, M., 2021. Optimized biological CO₂-methanation with a pure culture of
4
5 600 thermophilic methanogenic archaea in a trickle-bed reactor. *Bioresour. Technol.*
6
7 601 333, 125135. <https://doi.org/10.1016/j.biortech.2021.125135>
8
9 602 Tong, D., Farnham, D.J., Duan, L., Zhang, Q., Lewis, N.S., Caldeira, K., Davis, S.J.,
10
11 603 2021. Geophysical constraints on the reliability of solar and wind power
12
13 604 worldwide. *Nat. Commun.* 12, 6146. <https://doi.org/10.1038/s41467-021-26355->
14
15 605 [z](https://doi.org/10.1038/s41467-021-26355-)
16
17 606 Treu, L., Kougias, P.G., De Diego-Díaz, B., Campanaro, S., Bassani, I., Fernández-
18
19 607 Rodríguez, J., Angelidaki, I., 2018. Two-year microbial adaptation during
20
21 608 hydrogen-mediated biogas upgrading process in a serial reactor configuration.
22
23 609 *Bioresour. Technol.* 264, 140–147.
24
25 610 <https://doi.org/10.1016/j.biortech.2018.05.070>
26
27 611 Tsapekos, P., Alvarado-Morales, M., Angelidaki, I., 2022. H₂ competition between
28
29 612 homoacetogenic bacteria and methanogenic archaea during biomethantion from
30
31 613 a combined experimental-modelling approach. *J. Environ. Chem. Eng.* 10,
32
33 614 107281. <https://doi.org/10.1016/j.jece.2022.107281>
34
35 615 Vermeij, P., Pennings, J.L., Maassen, S.M., Keltjens, J.T., Vogels, G.D., 1997. Cellular
36
37 616 levels of factor 390 and methanogenic enzymes during growth of
38
39 617 *Methanobacterium thermoautotrophicum* deltaH. *J. Bacteriol.* 179, 6640–6648.
40
41 618 <https://doi.org/10.1128/jb.179.21.6640-6648.1997>
42
43 619 Wahid, R., Mulat, D.G., Gaby J.C., Horn, S.V., 2019. Effects of H₂:CO₂ ratio and H₂
44
45 620 supply fluctuation on methane content and microbial community composition
46
47
48
49
50
51
52
53
54
55
56
57
58
59
60
61
62
63
64
65

1 621 during *in-situ* biological biogas upgrading. *Biotechnol Biofuels* 12, 104.
2
3 622 <https://doi.org/10.1186/s13068-019-1443-6>
4
5 623 Wick, R.R., Judd, L.M., Gorrie, C.L., Holt, K.E., 2017. Unicycler: Resolving bacterial
6
7
8 624 genome assemblies from short and long sequencing reads. *PLOS Comput. Biol.*
9
10 625 13, e1005595. <https://doi.org/10.1371/journal.pcbi.1005595>
11
12 626 Xu, J., Bu, F., Zhu, W., Luo, G., Xie, L., 2020. Microbial Consortia of
13
14
15 627 Hydrogenotrophic Methanogenic Mixed Cultures in Lab-Scale Ex-Situ Biogas
16
17
18 628 Upgrading Systems under Different Conditions of Temperature, pH and CO.
19
20 629 *Microorganisms* 8, 772. <https://doi.org/10.3390/microorganisms8050772>
21
22
23 630
24
25 631
26
27
28
29
30
31
32
33
34
35
36
37
38
39
40
41
42
43
44
45
46
47
48
49
50
51
52
53
54
55
56
57
58
59
60
61
62
63
64
65

1 632 **Figure captions:**

2
3 633 **Figure 1: Relative abundance of microbial taxa inferred from Illumina MiSeq**

4
5
6 634 **sequencing of 16S rRNA genes. (A)** Archaeal abundance at the genus level from the

7
8 635 V4-V5 16S rRNA region of the 16S rRNA gene. The pie chart on right indicates

9
10 636 abundance of minor genera (<2% of total archaeal reads). **(B)** Bacterial abundance at

11
12 637 the phylum level from the V3-V4 16S rRNA region of the 16S rRNA gene. The pie

13
14 638 charts on right show the proportion of the different classes and genera constituting the

15
16
17
18 639 phyla *Bacillota* and *Pseudomonadota*.

19
20 640 **Figure 2: Comparative genomics of strain Clermont. (A)** Phylogenomic tree of

21
22 641 major archaeal clades based on a 73 genes core set using GToTree v1.8.2. **On left:**

23
24 642 Known major clades, including *Methanothermobacter* (dark pink) are collapsed and

25
26 643 shown as wedges of different colors. *Halobacteriales* was placed as outgroup. Bar, 0.3

27
28 644 substitution per amino acid position. **On right:** Decollapsed *Methanothermobacter*

29
30 645 wedge showing the position of strain Clermont (in red) within this genus. Bar, 0.05

31
32 646 substitution per amino acid position. **(B)** Collinearity analysis among assemblies of the

33
34 647 seven genomes forming the Marburg clade using MUMmer v4.0.0rc1 and visualized

35
36 648 using NGenomeSyn. **(C)** Anvi'o representation of the pan-genome of the Marburg

37
38 649 clade. Gene clusters (n = 2076) were ordered according to a hierarchical clustering of

39
40 650 their presence/absence (inner dendrogram). Rings show the presence (filled) or absence

41
42 651 (undashed) of the gene clusters in each genome. Single copy core and other core: gene

43
44 652 clusters present in all seven *Methanothermobacter* genomes. Gene clusters exclusively

45
46 653 present in a unique genome are indicated by a number: 1. strain K4, 2. strain THM_2, 3.

47
48 654 JZ-3_D_bin_25, 4. strain Kepco-1, 5. GMQ_75_MeOH_H2_bin_21, 6. strain Marburg,

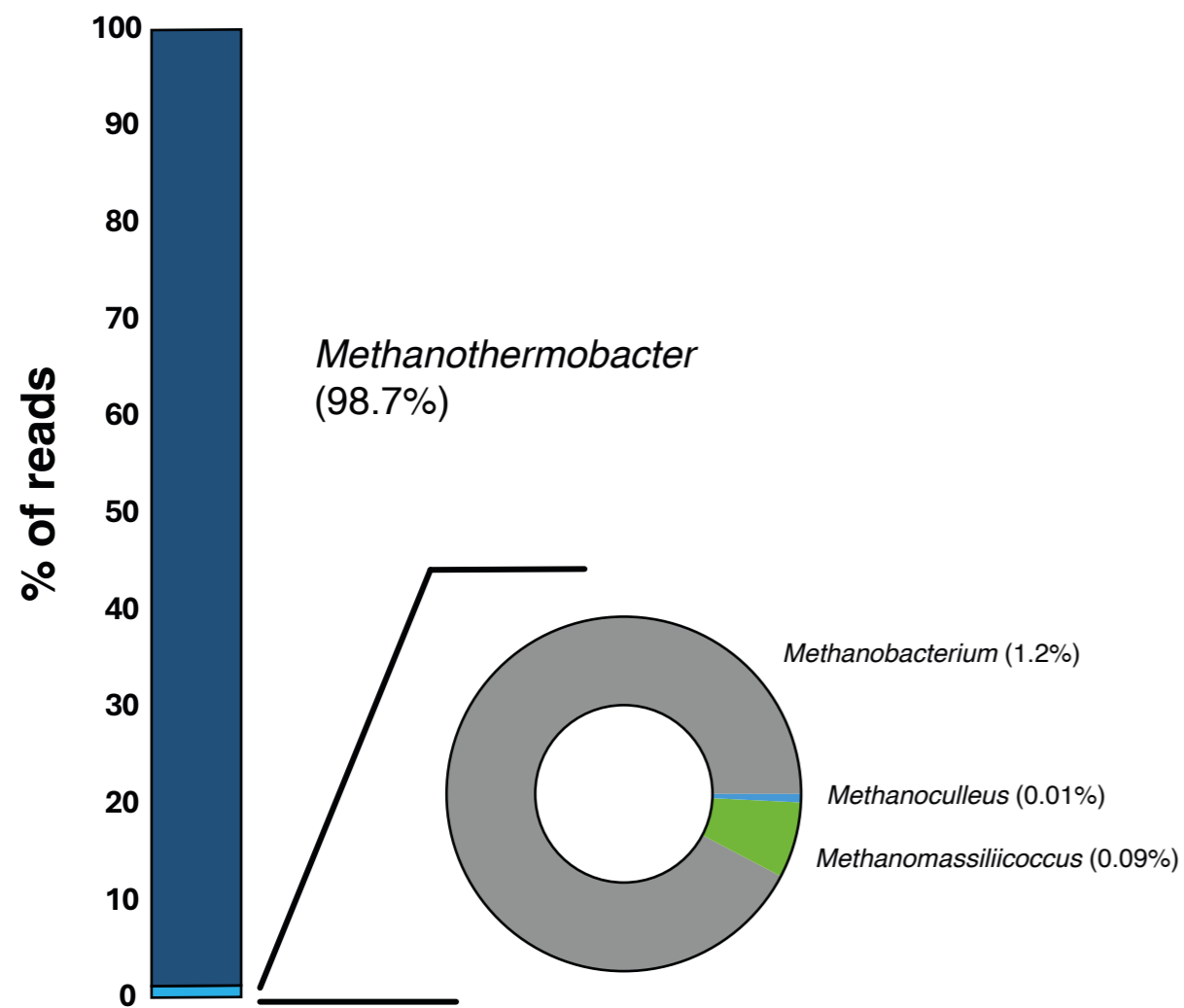
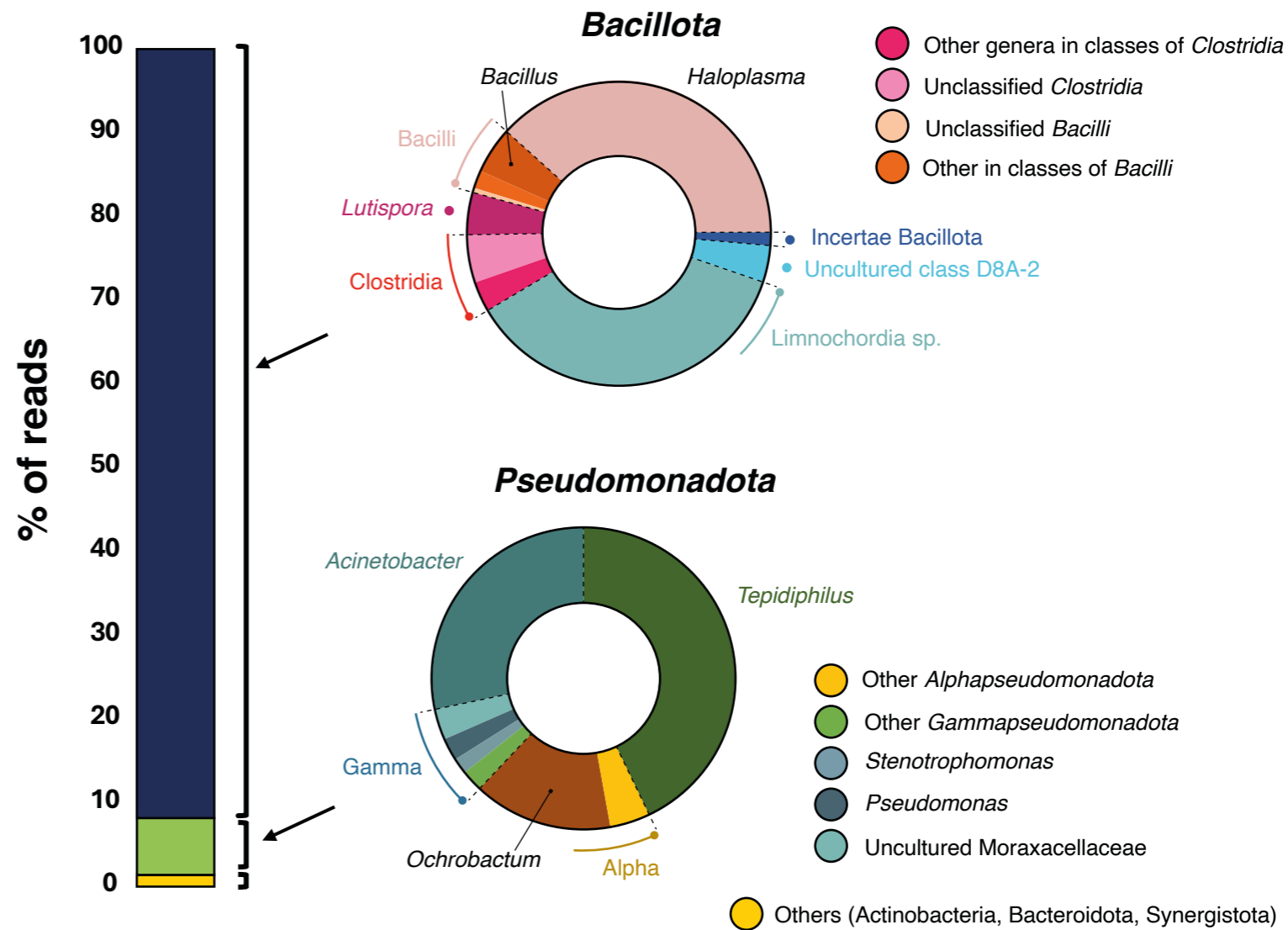
1 655 7. strain Clermont. To the right is given an ANI percentage identity heatmap; red: 100%
2
3 656 identity; light red: values ranging from 96% to 97%; white: values <96%.

4
5
6 657 **Figure 3: Methane yield under reduced conditions in batch culture for pure strains**
7
8 658 **(i.e. Marburg and Clermont) and the mixed adapted culture.** An asterisk denotes a
9
10 659 significant difference ($p < 0.05$) between strain Marburg versus the two other cultures
11
12
13 660 (days 3 to 6), and between the mixed culture versus pure cultures (days 8 and 18). The
14
15 661 error bar indicates the standard error (n=3).

16
17
18 662 **Figure 4: Methane yield in batch cultures under oxidative stressed conditions (240**
19
20 663 **min of exposure to O₂).** (A) Comparison over time between strain Clermont and mixed
21
22 664 adapted culture. (B) Comparison over time between strain Clermont and strain Marburg.
23
24 665 An asterisk denotes a significant difference ($p < 0.05$) between cultures over time. The
25
26 666 error bar indicates the standard error (n=3).

27
28
29
30 667 **Figure 5: Schematic representation of oxidative stress protection enzymes detected**
31
32 668 **in the Marburg clade genomes.** (A) Gene-loci in the genome of strain Marburg. (B)
33
34 669 Potential cellular responses to oxidative stress.

35
36
37 670
38 671
39
40
41
42
43
44
45
46
47
48
49
50
51
52
53
54
55
56
57
58
59
60
61
62
63
64
65

A**B**

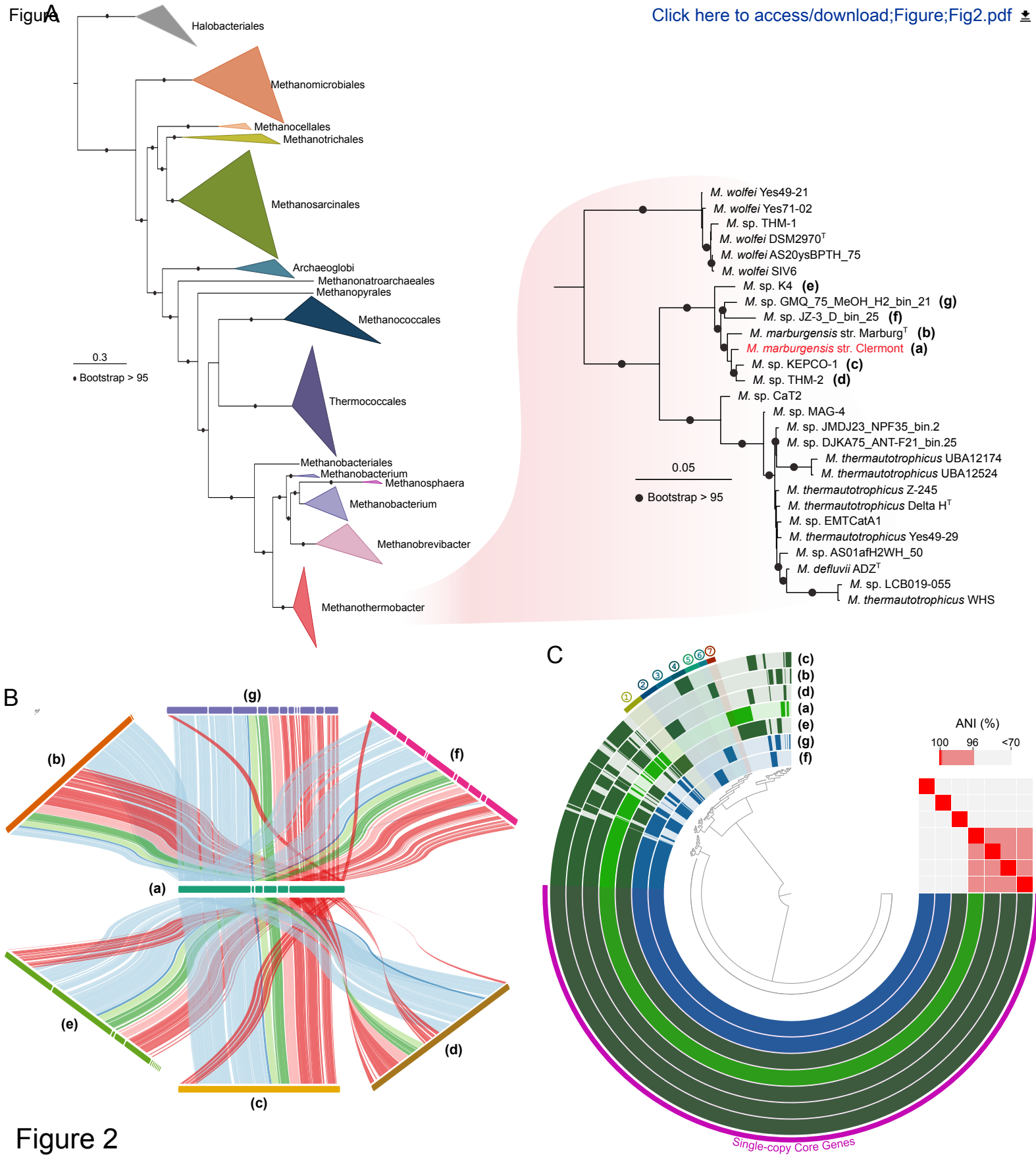


Figure 2

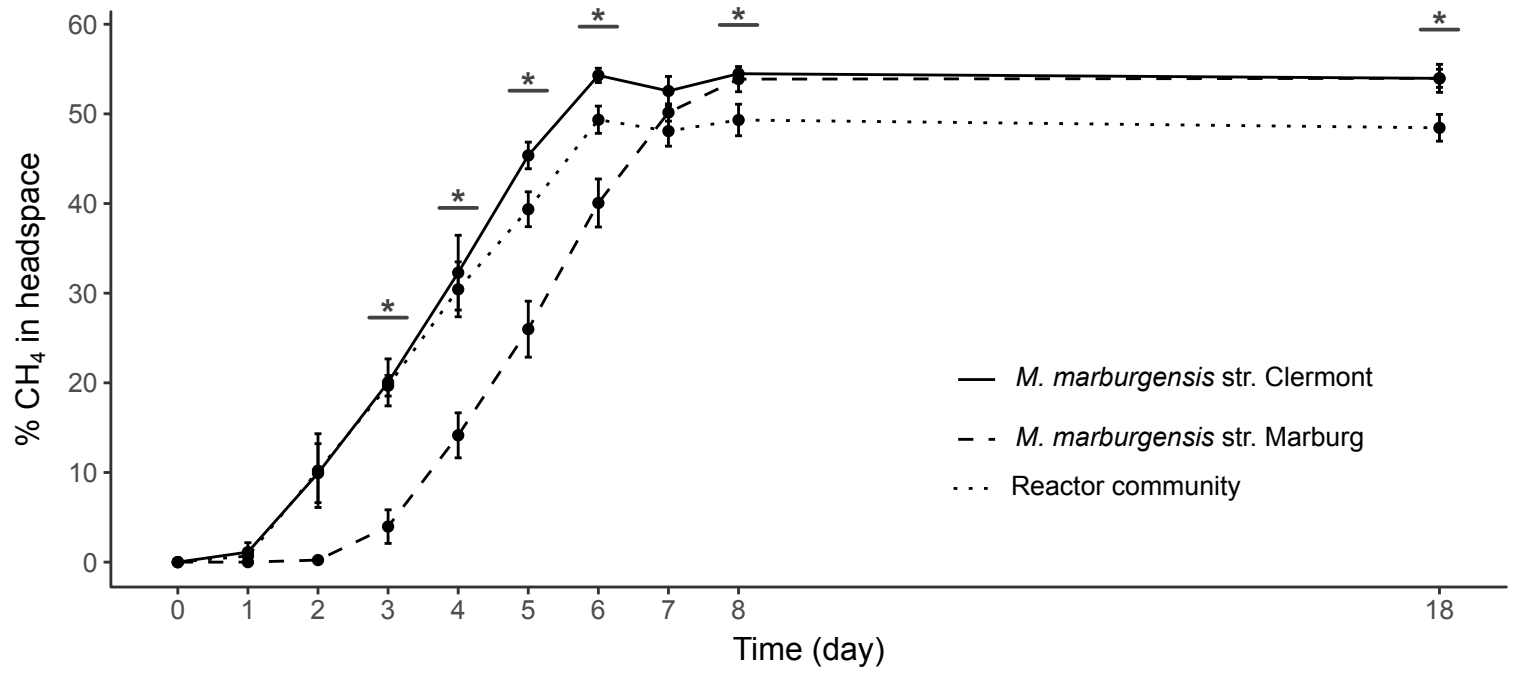


Figure 3

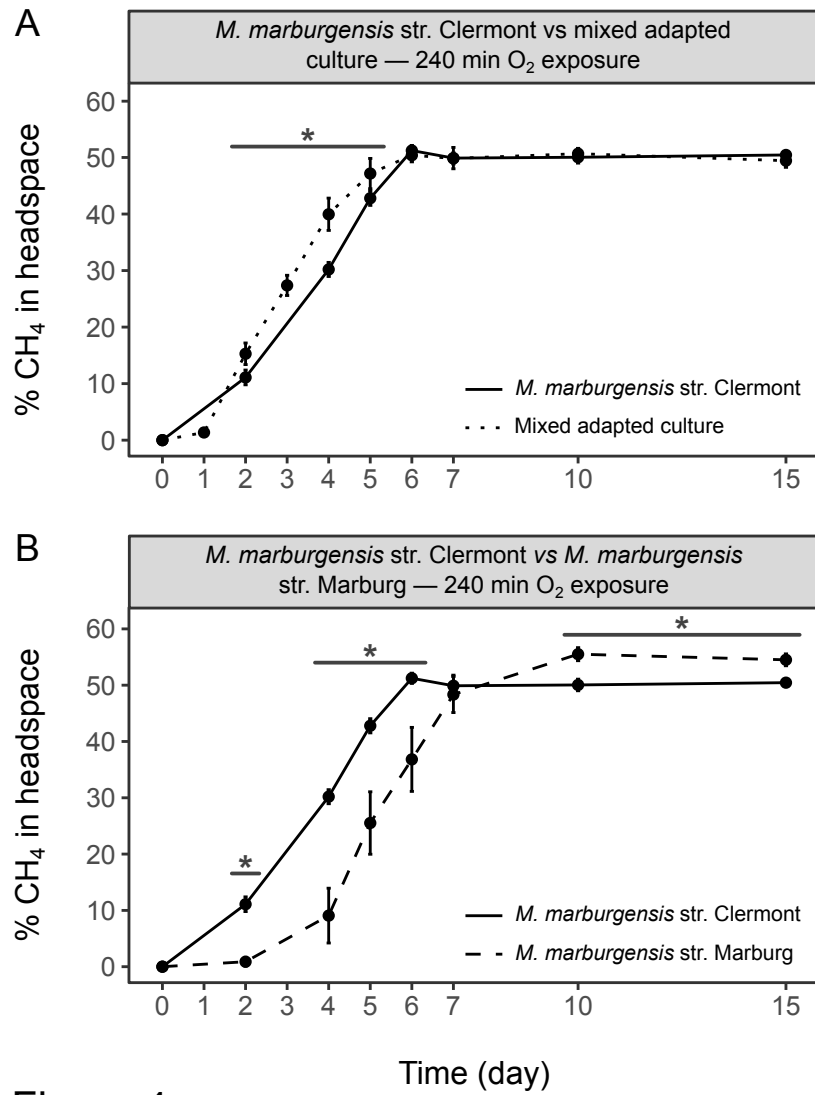
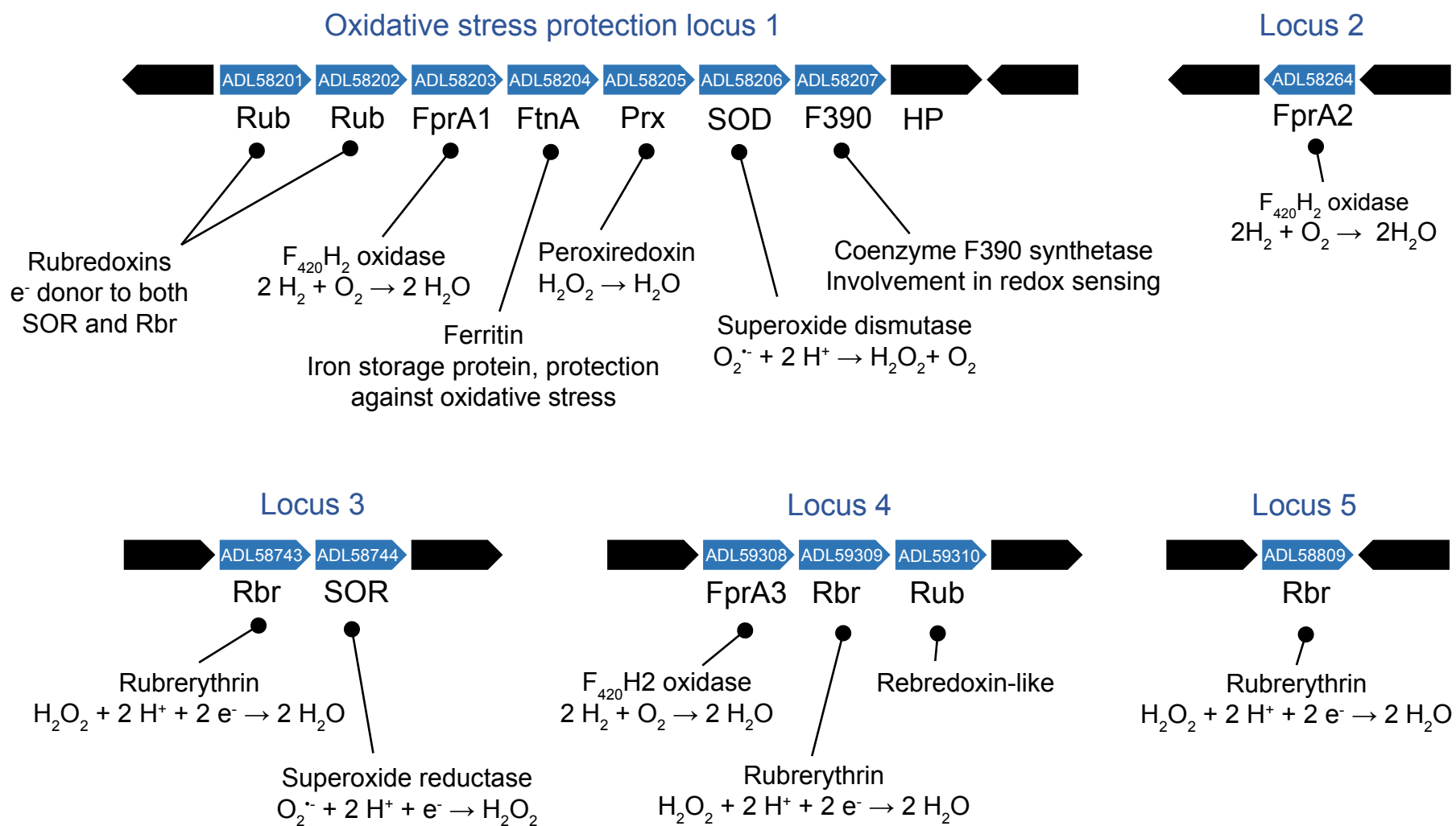


Figure A



B

O₂/ROS elimination

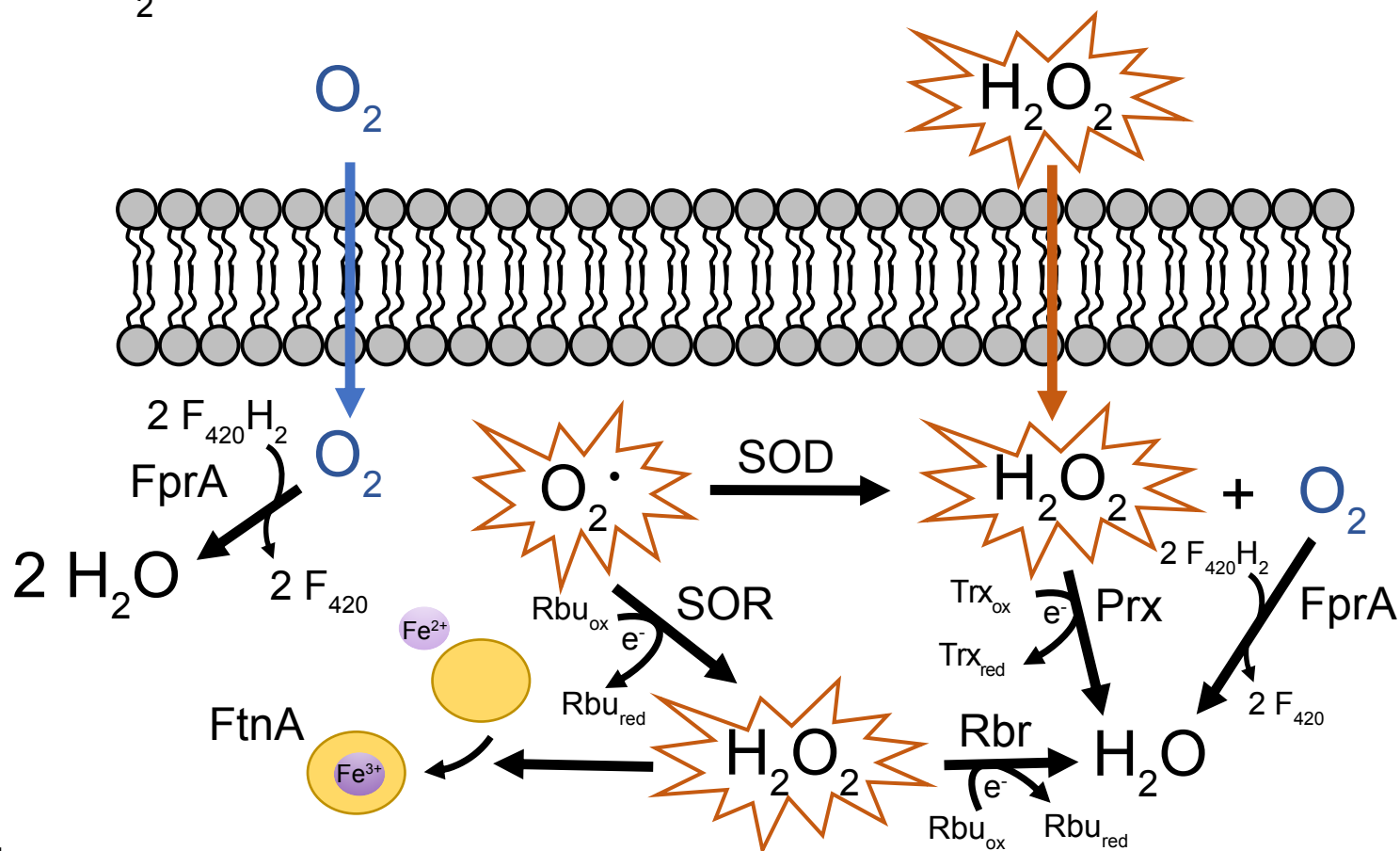


Figure 5

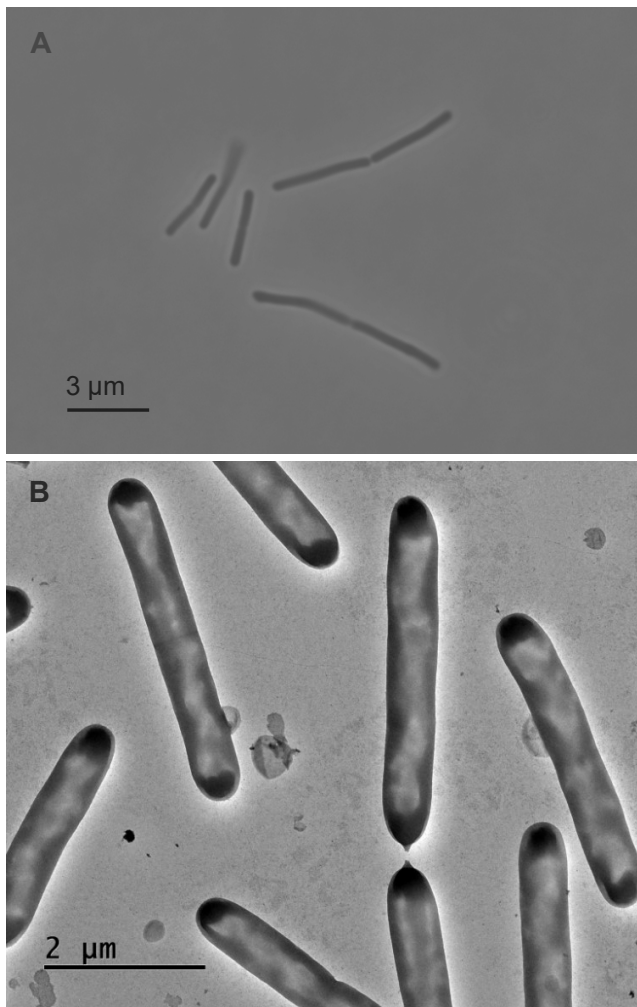


Figure S1: Morphology of *Methanothermobacter marburgensis* strain Clermont in optical microscopy (A) and transmission electron microscopy (B).

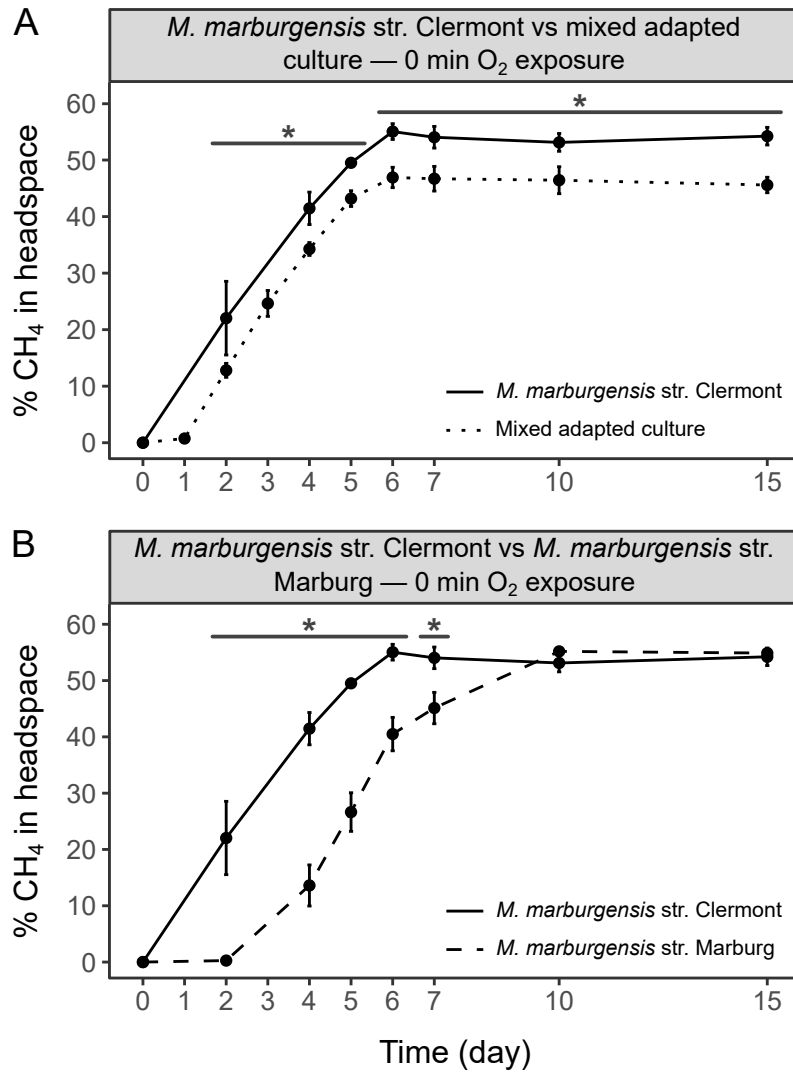
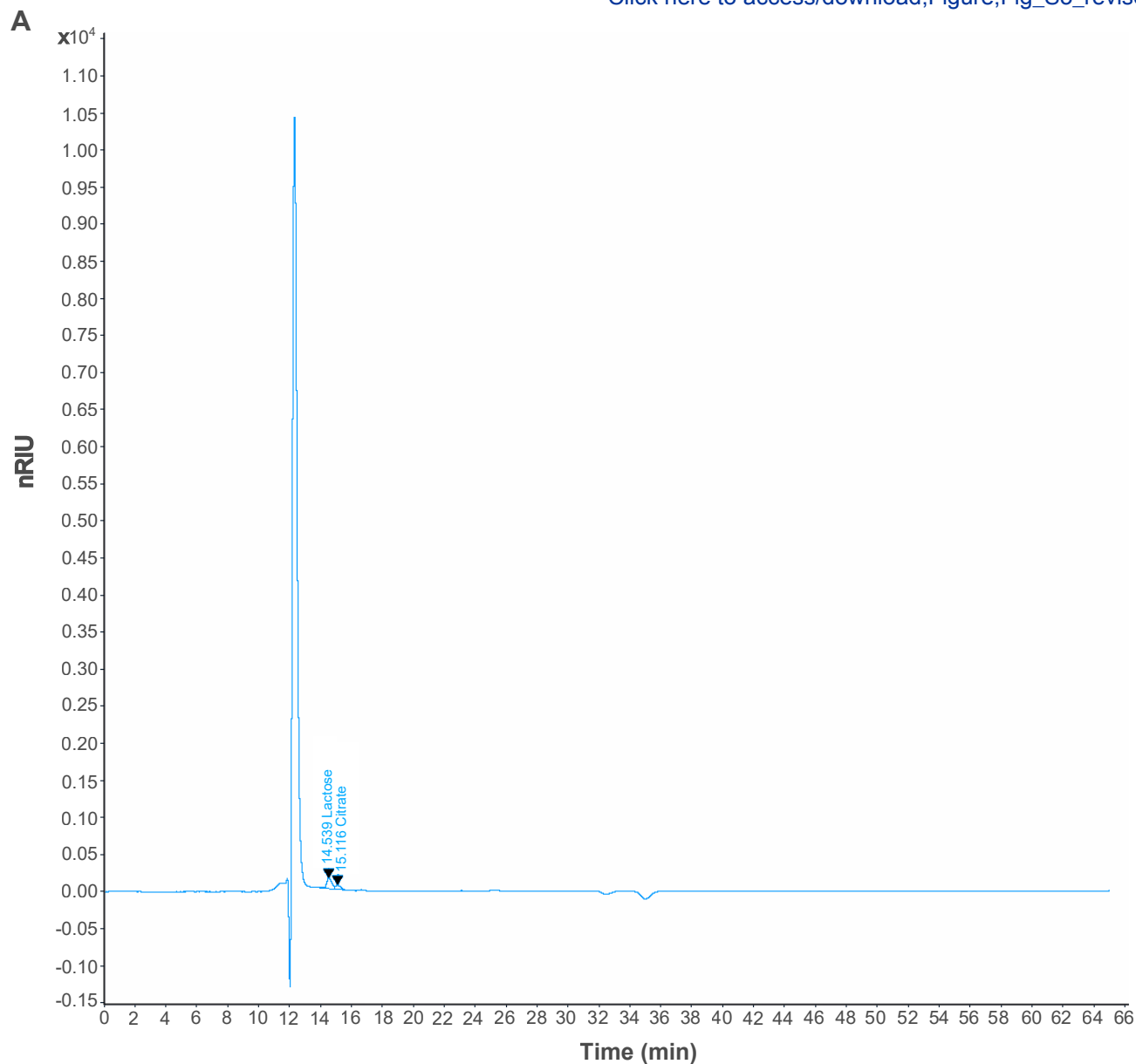


Figure S2: Methane production in batch cultures at the first level (0 min of exposure to O_2) of the experiment oxidative stressed conditions. (A) Comparison over time between strain Clermont and the mixed adapted culture. (B) Comparison over time between strain Clermont and strain Marburg. Asterisks denote a significant difference ($p < 0.05$) between cultures over time. The error bar indicates the standard error ($n=3$).



B

Age	Citrate	Lactate	Acetate	Propionate	Butyrate	Succinate	Ethanol	Lactose	Glucose
0	0.017	0	0	0.054	0	0	0	0.033	0
43	0.015	0	0	0.017	0	0	0	0.032	0
46	0.015	0	0	0	0	0	0	0.036	0
50	0.016	0	0	0	0	0	0	0.036	0
54	0.014	0	0	0	0	0	0	0.032	0

Figure S3: Organic acids, ethanol, lactose, and glucose concentrations measured by liquid chromatography in mixed adapted cultures. (A) Chromatogram for the six-week mixed adapted culture used in the study (age 46 days post inoculation of bubble column reactor with digestate sample). (B) Concentrations for mixed adapted cultures of different ages (0 to 54 days post inoculation) including that used in the study (in blue, 46 days).

Declaration of interests

The authors declare that they have no known competing financial interests or personal relationships that could have appeared to influence the work reported in this paper.

The authors declare the following financial interests/personal relationships which may be considered as potential competing interests:

Pierre Fontanille has patent #Procédé de biométhanation in situ Number FR2211561 pending to neither licensee nor assignee. The authors declare that the strain *Methanothermobacter marburgensis* strain Clermont presented in this work was deposited according to the Budapest Treaty (rule 11.2, option 1) for the purposes of patent (filed on 7 november 2022). The authors declare that they have no known competing interests. If there are other authors, they declare that they have no known competing financial interests or personal relationships that could have appeared to influence the work reported in this paper.